Diploma Thesis

Impact of FGF21 on tissue signaling & metabolism

submitted by

Lena Elisabeth Voško

in partial fulfillment of the requirements for the degree of

Doktorin der gesamten Heilkunde

(Dr^{in}. med. univ.)

at the

Medical University of Graz

executed at the

University departments of Internal Medicine

Division of Gastroenterology and Hepatology

under the supervision of

Tarek Moustafa, Univ.-Ass. Mag. Dr.rer.nat.

Peter Fickert, Univ.-Prof. Dr.

Graz, January 31, 2024

Declaration of Academic Integrity

I hereby confirm that the present diploma thesis is the result of my own independent scholarly work. I also confirm that in all cases, where material from the work of others (in books, articles, essays, dissertations, and on the internet) is acknowledged, quotations and paraphrases are clearly indicated. No material other than that cited in the reference list has been used. I have read and understood the Medical University's regulations and procedures concerning plagiarism.

Graz, January 31,2024 Lena Elisabeth Voško m.p.

ACKNOWLEDGMENTS

First of all, I would like to express my gratitude to my supervisor Univ.-Ass. Dr. Tarek Moustafa for giving me the opportunity to work on this diploma thesis, supporting and guiding me over the years and awakening my fascination for science and research. Furthermore, I would like to thank Professor Peter Fickert for his support and for giving me the great chance to work at his research group.

I would like to extend my appreciation to Martin Vargek, who taught me critical thinking and organization, and who was always there for help. Thank you for teaching me how to work in a lab and for making science fun!

A huge thank you goes also to Dagmar, Judith, Katrin, Michelle and Sylvia, who always offered a helpful hand and made my time in the lab very special.

My heartfelt appreciation goes to my husband Ivan for listening to my problems and working with me on solutions and to my friends and family, for the greatest mental support.

Last but not least, I would like to express my deepest gratitude for my parents, who were supporting me throughout my life. Your encouragement and understanding provided me with everything I needed, for which I am very grateful!

ZUSAMMENFASSUNG

Fibroblast Growth Factor 21 (FGF21) ist ein endokrines Polypeptid und Teil der atypischen FGF 15/19-Unterfamilie. Im Gegensatz zu den anderen FGFs ist diese Gruppe in der Lage durch den Blutkreislauf zu wandern und somit an anderen Organen zu wirken und wie im Fall von FGF21, positive metabolische Effekte wie Gewichtsreduktion und Kontrolle des Blutzuckerspiegels zu erzeugen. FGF21 wird hauptsächlich in der Leber produziert und sekretiert. Auch wenn Zusammenhänge zwischen FGF21 und Metabolismus in Leber und Fettgewebe schon in Studien untersucht wurden, gab es in diesem Feld bis dato noch keine Arbeiten zum Thema *ex vivo* Effekte in Explantkulturen.

Diese Diplomarbeit beschäftigte sich mit einem neu-modifizierten Maus-FGF21 (modFGF21) und testete seine Wirkungsweise in Zellkulturen und Fettgewebsexplantaten. Darüber hinaus wollten wir zeigen, dass Fettgewebsexplantate ähnlich der Nutzung von Zellen in Kultur für die weitere Forschung eingesetzt werden können, um an Signalkaskaden von FGF21 zu forschen.

HUH7-Zellen wurden mit verschiedenen Ansätzen modFGF21s behandelt. Um die Funktionsfähigkeit der Fettgewebsexplantate zu testen, wurde inguinales und gonadales weißes Fettgewebe aus C57BL/6-Mäusen entnommen und mit FGF21, Isoproterenol oder Insulin behandelt. Wir erprobten verschiedene Medien, Therapiekonzentrationen und Behandlungsdauern. Anschließend ermittelten wir mithilfe der Westernblot-Technik das Niveau von FGF21-Schlüsselproteinen, die für Signalkaskaden im Fettstoffwechsel und FGF21-abhängigen Metabolismus verantwortlich sind und maßen ein Schlüsselgen der FGF21-Signalwirkung mittels RT-qPCR.

Bei der Behandlung von HUH7-Zellen mit modFGF21 kam es zu erhöhten Proteinmengen der phosphorylierten extracellular-signal regulated kinase (pERK1/2). Die Stimulation der Fettgewebsexplantaten mit Isoproterenol oder Insulin führte zu erhöhten Proteinleveln der phosphorylierten hormon-sensitiven Lipase (pHSL) sowie phosphorylierten Proteinkinase B (pAkt). Es konnten jedoch

nach Behandlung mit FGF21 keine erhöhten Proteinlevel der pERK1/2 detektiert werden.

Wir konnten hiermit zeigen, dass Fettgewebsexplantate zur weiteren Forschung an Signalwirkungen im Lipidstoffwechsel angewendet werden können, doch es braucht weitere Studien, um in diesem Modell auch die Wirkungsweise von FGF21 untersuchen zu können.

ABSTRACT

Fibroblast growth factor 21 (FGF21) is a polypeptide hormone and member of the atypical FGF 15/19 subfamily. In contrast to other FGFs, members of the FGF 15/19 subfamily are endocrine peptides, able to travel through the blood stream. FGF21 is mostly produced and secreted by the liver and is known for its beneficial metabolic effects regarding weight loss and glycemic control. We developed a modified murine FGF21 (modFGF21) that should show a higher formulation stability for future scientific use in mouse models. Although FGF21 research has illuminated a variety of effects on metabolism in liver and adipose tissue, no study to date has examined these relations in cell culture and organ explants with our newly developed modFGF21. This diploma thesis was designed to test the performance of modFGF21 on cell culture and adipose organ explants from mice. Furthermore, this work assesses the hypothesis that organ explant culture can be utilized to demonstrate effects of FGF21 signaling.

HUH7 cells were treated with different stocks of modFGF21 to test the performance on cell culture. In order to test the suitability of the adipose-tissue- organ explant culture, we extracted gonadal and inguinal white adipose tissue from C57BL/6 mice and treated with FGF21, isoproterenol or insulin. We tried out different treatment concentrations, media and treatment durations. To determine the impact of FGF21 signaling and lipolysis signaling we measured levels of key proteins using Western blot analysis and expression levels of key genes using RT-qPCR.

Treatment of HUH7 cells with our modified murine FGF21 led to higher protein levels of phosphorylated extracellular-signal regulated kinases (pERK1/2). Stimulation of the explanted adipose tissue with isoproterenol and insulin led to elevated protein levels of phosphorylated hormone-sensitive lipase (pHSL) and phosphorylated protein kinase B (pAkt), respectively, both representing well-established downstream targets. However, there was no difference in pERK1/2 protein levels in explanted adipose tissue treated with modFGF21 or recombinant purified FGF21, compared to vehicle.

We could demonstrate that organ explant culture based on adipose tissue can be utilized to test different signaling cascades in lipid metabolism. Nevertheless, FGF21 could not induce a clear induction of pERK1/2 in adipose explant cultures, therefore new investigations are needed to develop a system that can be applied to FGF21.

PUBLICATIONS

No publications have been issued or released.

TABLE OF CONTENTS

LIST OF ABBREVIATIONS

AMPK	5' adenosine monophosphate-activated protein kinase
ACLY	adenosine triphosphate citrate lyase
APS	ammonium persulfate aps
ANF	atrial natriuretic factor
BBB	blood-brain barrier
BSA	bovine serum albumin
BAT	brown adipose tissue
ChREBP	carbohydrate responsive element binding protein
CNS	central nervous system
csFBS	charcoal-stripped fetal bovine serum
cDNA	complementary deoxyribonucleic
dNTP	deoxynucleotide triphosphates
dFBS	dialyzed fetal bovine serum
DIO	diet-induced obese
DPPIV	dipeptidyl peptidase IV
dH20	distilled H20
DTT	dithiothreitol
DMEM	dulbecco’s modified eagle medium
EGR-1	early growth response-1
ER	endoplasmic reticulum
EDTA	ethylenediaminetetraacetic acid
ERK1/2	extracellular signal-regulated kinase 1/2
FBS	fetal bovine serum
FGFR	fibroblast growth factor receptor
FAP	fibroblast activation protein
FGF	fibroblast growth factor
FGF21	fibroblast growth factor 21
FRS2α	fibroblast growth factor receptor substrate 2 alpha
FFA	free fatty acids
gWAT	gonadal white adipose tissue
HSGAG	heparan sulfate glycosaminoglycans
HCC	hepatocellular cancer

HDL	high density lipoprotein
HB	homogenization buffer
HSL	hormone-sensitive lipase
hFGF21	human fibroblast growth factor 21
HCL	hydrochloric acid
HPA	hypothalamic-pituitary-adrenal axis
iWAT	inguinal white adipose tissue
IL-6	interleukin-6
JMJD3/KDM6B	jumonji-d3 histone demethylase
KO	knockout
LDL	low density lipoprotein
LY	LY2405319
MASH	metabolic dysfunction-associated steatohepatitis
MASLD	metabolic dysfunction-associated steatotic liver disease
mRNA	messenger ribonucleic acid
MAPK	mitogen-activated protein kinase
mFGF21	murine fibroblast growth factor 21
modFGF21	modified mice fibroblast growth factor 21
MCP-1	monocyte chemoattractant protein-1
MSG	monosodium glutamate
BIS	N,N-methylenbis-acrylamide
NAD^+	nicotinamide adenine dinucleotide$^+$
Ob	obese
BMS-986036	pegbelfermin
PGC-1α	peroxisome proliferator-activated receptor λ coactivator protein 1-alpha
PPARalpha	peroxisome proliferator-activated receptor alpha
PBS	phosphate buffered saline
p-	phospho-
PEG	polyethylene glycol
PPI	protease and phosphatase inhibitors
PKA	protein kinase a
Akt	protein kinase b

ROS	reactive oxygen species
RNA	ribonucleic acid
Sirt-1	sirtuin-1
SDS	sodium dodecyl sulfate
s	standard
SEM	standard error of the mean
TBS-T	tris-buffered saline-tween
TEMED	tetramethylethylenediamine
TAG	triacylglycerol
TBS	tris-buffered saline
TRIS	tris(hydroxymethyl)aminomethane
TH	tyrosine hydroxylase
UXT	ubiquitously expressed prefoldin like chaperone gene
WAT	white adipose tissue
WR	working reagent
α-SKA	α-skeletal actin
KLB	β-klotho

LIST OF FIGURES

LIST OF TABLES

1. INTRODUCTION

1.1. Fibroblast growth factors

Fibroblast growth factors (FGFs) are polypeptides that bind to specific FGF receptor tyrosine kinases (FGFRs) (Ornitz and Itoh, 2001). FGFs play important roles in the embryonic period, as well as in the adult stage of both humans and animals. Their functions include the regulation of cell development such as cell migration, differentiation and proliferation. Additionally, they work as homeostatic factors and are involved in tissue injury and repair (Ornitz and Itoh, 2001). There are 18 mammalian FGFs (FGF 1-10 and FGF 16-23) and four FGFRs (FGFR 1-4). The FGF family is divided into five paracrine groups and one endocrine group (Beenken and Mohammadi, 2012). The FGF 1 subfamily consists of FGF 1 and 2; the FGF 7 subfamily consists of 3, 7, 10 and 22; the FGF 4 subfamily contains FGF 4, 5, 6; the FGF 8 subfamily contains FGF 8, 17 and 18; and the FGF 9 subfamily contains 9, 16 and 20. All of them act solely in a paracrine way whereas the FGF 19 subfamily, which contains FGF 19, 21 and 23, can act in an endocrine manner as well (Beenken and Mohammadi, 2012). Counting all human and mice FGFs, there is a number of 22 different members (Fon Tacer et al., 2010). Notably, FGF 15 is the mouse homologue of human FGF 19. The majority of the previously mentioned FGFs bind to the heparan sulfate glycosaminoglycans (HSGAGs) with a high affinity, which can be found on the cell membrane or in the extracellular matrix. Only the FGF 15/19 subfamily behaves differently. The members are called atypical FGFs because of their poor binding affinity to the HSGAGs. They are thus able to work as endocrine peptides and travel through the blood stream (Fon Tacer et al., 2010). The existence of the so-called klotho proteins (alpha-klotho or beta-klotho) in target tissue seems to play an important role in why they behave in an endocrine way. To increase the ligand-receptor affinity of the FGF/FGFR complex, klotho proteins are necessary for the connection between the two players (Beenken and Mohammadi, 2009).

The key organ for the secretion of FGF19 is the ileum. The highest expression of FGF19 is observed after food intake (Talukdar and Kharitonenkov, 2021). FGF19

acts as a regulator of bile acid homeostasis and glucose during the fed-to-fasted state shift (Gadaleta and Moschetta, 2019), whereas Vitamin D and phosphate metabolism is partially controlled by FGF23, a protein with the highest expression in bone (Beenken and Mohammadi, 2009).

1.2. Fibroblast growth factor 21

In the year 2000, Fibroblast Growth Factor 21 (FGF21) was described for the first time by Nishimura and colleagues in Japan. With the help of cDNA isolation, they identified the new member of the FGF-subfamily in different mice and human tissues (Nishimura et al., 2000).

FGF21 is mainly produced and secreted in the liver. However, there is evidence that production, although in smaller amounts, can occur in other tissue such as pancreas, muscle and adipose tissue. Fasting conditions and ketogenic diet induce the production and secretion of FGF21 in hepatocytes of mice and humans (Badman et al., 2007, Inagaki et al., 2007)

1.2.1. Structure and Signaling

The molecular weight of FGF21 is 20 kDa with a total number of 181 amino acids, of which 75% are shared between mice and humans (Henriksson and Andersen, 2020, Flippo and Potthoff, 2021). The FGF21 gene shows approximately 75% similar sequences between vertebrate species and thus classifies as highly conserved (Szczepanska and Gietka-Czernel, 2022).

Like the other FGFs, FGF21 has a structurally conserved central core with an atypical b-trefoil topology, which is necessary for binding to the FGFRs (Luo et al., 2019). After secretion of FGF21 from the cell, the protein activates the signaling cascade by binding to the complex of the co-receptor β-klotho (KLB) and the receptor FGFR1c, the traditional receptor of FGF21 with the highest affinity for the protein (Suzuki et al., 2008, Adams et al., 2012a). Whereas FGFR1c shows a high

expression in most tissues, KLB is limited to only enterohepatic tissues such as liver, gall bladder and pancreas, as well as brown and white adipose tissues (Fon Tacer et al., 2010). Additionally, Angie L. Bookout and colleagues have found that in the presence of KLB in hypothalamus and hindbrain, FGF21 can affect the adaptive starvation response in the central nervous system (Bookout et al., 2013). In different experiments, researchers have demonstrated that the absence of KLB *in vitro* and *vivo* leads to a missing effect of FGF21 signaling (Adams et al., 2012a, Suzuki et al., 2008, Kurosu et al., 2007).

With the help of X-ray crystallography, in 2017 Sangwon Lee and colleagues looked at the structure of human KLB to understand the action of KLB in FGF21 cell signaling. KLB, a cell-surface protein with tandem glycosidase domains, is described as a primary 'zip code'-like receptor or targeting signal for FGF21 because of its direct interaction with the C-terminus of FGF21. Therefore, KLB is necessary for binding and activation of the effector receptor FGFR (Lee et al., 2018). After examining the N- and C-termini of FGF21 using 293T cells in a luciferase reporter assay system, Junming Yie and colleagues have shown that the C-terminus of FGF21 plays an important role for the binding of KLB, whereas the N-terminus is significant for FGFR activation. After deletion of the C-terminus, they detected a potency loss in the assay and after deletion of the N-terminus, the result was a reduction of maximal response, or a partial agonistic effect. It is unknown how the interaction between FGF21/FGFR1c works exactly, however, direct interaction has not been demonstrated (Yie et al., 2009).

In cell experiments, M. Mohammadi and colleagues have confirmed that FGFR1 has seven different autophosphorylation sites (tyrosine 766, Y-463, Y-583, Y-585, Y-653, Y-654 and Y-730). They have identified the crucial role of the tyrosines 653 and 654 in stimulating the tyrosine kinase of FGFR1 (Mohammadi et al., 1996).

A study from Alexei Kharitonenkov and colleagues has revealed the effect of FGF21 signaling in 3T3-L1 adipocytes. When forming the FGF21/FGFR1/KLB-complex, there is activation of the intracellular tyrosine kinase of FGFR1 and furthermore, phosphorylation of the extracellular signal-regulated kinase (ERK), a member of the mitogen-activated protein kinase (MAPK) family (Kharitonenkov et al., 2005). After

activation of ERK by FGF21/FGFR1/ KLB signaling, the receptors are internalized by endocytosis (Yaqoob et al., 2014). Despite some studies regarding post-translational protein modifications and altered gene expression, detailed insights into the intracellular signaling process of FGF21 are lacking (Flippo and Potthoff, 2021).

In a further trial, Mary D.L. Chau and colleagues have registered higher phosphorylated AMPK levels in 3T3-L1 adipocytes after treatment with FGF21. In addition, studies have uncovered an increase in NAD^+ metabolism and Sirtuin-1 activity (Chau et al., 2010), relevant factors in mitochondrial metabolism and antioxidative protection (Canto and Auwerx, 2012) .

Matthew J. Potthoff and colleagues have demonstrated the impact of FGF21 regarding the hepatic peroxisome proliferator-activated receptor λ coactivator protein 1-alpha (PGC-1α) expression. In transgenic FGF21-mice, they have shown a 5-fold higher increase of hepatic *Pgc-1α,* compared to hepatic *Pgc-1α* in wildtype mice. PGC-1α plays a key role in the transcriptional regulation of energy homeostasis and leads to elevation in fatty acid oxidation, tricarboxylic acid cycle flux and gluconeogenesis (Potthoff et al., 2009).

In a trial from Sangwon Byun and colleagues the role of FGF21 signaling in the activation of autophagy and lipid degradation has been demonstrated. In animal models with mice, they have discovered that Jumonji-D3 (JMJD3/KDM6B) histone demethylase is crucial for the epigenetic activation of the mentioned functions and that JMJD3 expression increases under administration of FGF21 in fasted mice (Byun et al., 2020).

The identified enzymes responsible for cleavage of FGF21 are fibroblast activation protein (FAP) and dipeptidyl peptidase IV (DPPIV). The endopeptidase FAP inactivates human FGF21 but interestingly, cannot cleave FGF21 in mice because of a single amino acid difference (Flippo and Potthoff, 2021, Dunshee et al., 2016).

1.2.2. Liver

In the liver, high expression of *FGF21* was found under specific diets including starvation, amino acid restriction and high-fat diet. Other reasons for increased expression were stress through exercise, oxidative stress and lipopolysaccharides (Kaur et al., 2022). Already in 2009, Iizuka and colleagues discovered the potential of FGF21 in metabolic physiology. In animal experiments with mice, glucose stimulation upregulated *FGF21* expression via ChREBP, a glucose activated transcription factor (Iizuka et al., 2009). Another key regulator of *FGF21* expression is peroxisome proliferator-activated receptor alpha (PPARalpha), a part of the nuclear receptor superfamily of ligand-activated transcription factors and regulator of lipid metabolism and insulin sensitivity (Haluzík and Haluzík, 2006). In a study from Inagaki and colleagues PPARalpha could directly activate *FGF21* expression under fasting conditions in mouse liver and human hepatocytes. Further, Inagaki has demonstrated that FGF21 activates ketogenesis and lipolysis in a PPARalpha dependent manner by showing the deficiency of these metabolic pathways in fasted PPARalpha-knockout mice (Inagaki et al., 2007). In a detailed trial, Fisher and colleagues have performed intraperitoneal FGF21 injections on mice which led to higher expression of important genes involved in mechanisms for gluconeogenesis such as *peroxisome proliferator-activated receptor-gamma coactivator (PGC)-1alpha,* and of genes for lipolysis and ketogenesis (Fisher et al., 2011). In different experiments with mice, FGF21 injections in diet-induced obese (DIO) and lean mice led to lower fatty acid levels, reduced hepatic triglycerides and improved insulin sensitivity (Xu et al., 2009a). Nevertheless, the most important receptor for FGF21-signaling *FGFR1* has a very low expression in liver tissue (Yang et al., 2012) which questions the paracrine function of FGF21 in the liver itself and presents a novel theory indicating that there is an unknown indirect pathway of FGF21 signaling (She et al., 2022).

1.2.3. Adipose tissue

Adipose tissue contains KLB and FGFR, the latter of which mainly shows expression of FGFR1 and FGFR2 in adipocytes (Suzuki et al., 2008). FGF21 shows different effects regarding white adipose tissue (WAT) and brown adipose tissue (BAT). BAT

has an important role in thermogenesis and is mediating metabolism and energy expenditure (Scheele and Wolfrum, 2020) Chartoumpekis and colleagues have shown that short-term cold exposure and β-adrenergic stimulation influence the expression of *FGF21* mRNA in BAT (Chartoumpekis et al., 2011). Cell culture and animal experiments demonstrated that FGF21 improves glucose uptake in BAT in the presence of insulin (BonDurant et al., 2017, Markan et al., 2014). WAT is mainly known for its function as energy storage (Saely et al., 2012). A recent study has revealed that the positive effects of FGF21 signaling on weight loss and energy expenditure in obese mice were markedly reduced in WAT-specific KLB/FGFR1 knock-out mice. The same paper has demonstrated that WAT in obese mice treated with long-term high-fat diet expresses less KLB and FGFR1 and therefore, does not respond to FGF21 (Geng et al., 2019). Previous research showed that FGF21 increases glucose uptake in T3-L1 cells and human adipocytes (Badman et al., 2007, Kharitonenkov et al., 2005). In multiple studies, FGF21 treatment reduced plasma glucose concentration (Suzuki et al., 2008, Kharitonenkov et al., 2005, Berglund et al., 2009), and therefore, FGF21 seems to have hypoglycemic effects on adipose tissue. Besides the blood glucose, FGF21 lowered insulin concentration in different obese or diabetic mice models (Kharitonenkov et al., 2005) which provides evidence that FGF21 has also an insulin sensitizing effect. Furthermore, FGF21 can diminish lipolysis and concentration of FFA in blood, which could be a cause for its insulin sensitizing effect (Arner et al., 2008). Interestingly, in *FGF21*-transgenic mice, lipolysis was decreased, and subcutaneous adipocytes were smaller in contrast to normal control mice (Kharitonenkov et al., 2005, Inagaki et al., 2007). In comparison, *FGF21*-knockout mice demonstrated less lipolysis and FFA levels in blood (Hotta et al., 2009).

1.2.4. Central nervous system

In the year 2007, Hung Hsuchou and colleagues demonstrated that FGF21 is able to cross the blood-brain barrier (BBB) (Hsuchou et al., 2007). KLB and FGFRs are expressed in the central nervous system (CNS), the hypothalamus, brain stem and hindbrain. Consequently, FGF21 could activate its signaling pathway in the brain (Lan et al., 2017, von Holstein-Rathlou et al., 2016). A study from 2014 proved that

under fasting conditions, FGF21 acts on the CNS by affecting the hypothalamic-pituitary-adrenal (HPA) axis which results in the stimulation of hepatic gluconeogenesis through secretion of corticosterone (Liang et al., 2014). Experiments with intracerebroventricular injections of FGF21 in mice have demonstrated the effect of FGF21 on the CNS. The treatment changes energy expenditure and leads to weight loss in obese mice by browning of WAT through the action of corticotropin-releasing factor. Based on that evidence, FGF21 could also affect sympathetic nerves (Owen et al., 2014). The effects of FGF21 on the CNS can change depending on the metabolic state of the animals. In fasting conditions, *KLB* expression decreases so that FGF21 signaling and the corresponding effects on the CNS are reduced (Matsui et al., 2018).

Food intake and nutrition play a notable role in the relationship between FGF21 and the CNS. Experiments with mice demonstrate that the absence of FGF21 increases sugar intake, concluding that FGF21 has an impact on sweet-taste preference in animals (von Holstein-Rathlou et al., 2016). Similar research findings claim that a higher intake of sugar causes higher *FGF21* expression (von Holstein-Rathlou et al., 2016) dependent on the transcription factor ChREBP (Iroz et al., 2017). Because of these findings, first trials have already proven that FGF21 mimetics reduce sweet taste preference and carbohydrate intake in obese patients (Baruch et al., 2020).
But not only carbohydrates play a role in FGF21 signaling. A recent study by Laeger et al has shown increased *FGF21* expression in conditions with a low protein diet in rodents and humans. The researchers concluded that FGF21 is an endocrine signal that mediates the behavioral and metabolic responses to protein restriction. Notably, carbohydrates as well as proteins require PPARα for the signaling pathway to increase *FGF21* expression (Laeger et al., 2014).

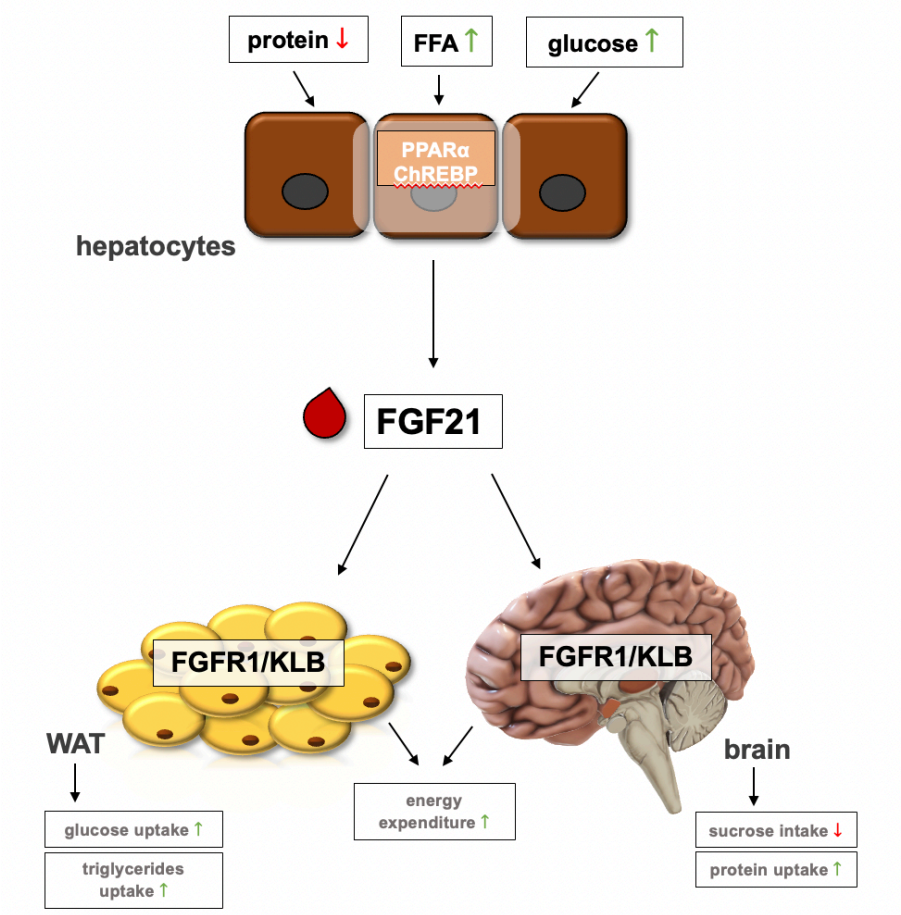

Figure 1: Regulation and effect on FGF21
adapted from (Henriksson and Andersen, 2020)

1.2.5. Heart

Especially in the past decade, scientists discovered the potential of FGF21 signaling in the heart. Researchers have already described the anti-oxidative, anti-hypertrophic and anti-apoptotic functions of FGF21 under physiological and pathological conditions (Kim and Lee, 2015, Itoh and Ohta, 2013).

In a trial from 2013, Shu Q. Liu and colleagues investigated the beneficial effect of FGF21 in mice models by performing myocardial ischemia/reperfusion injury. The expression of FGF21 was increased in myocardial ischemia. Furthermore, FGF21 has been shown to protect the heart and reduce the degree of myocardial infarction in short- and long-term experiments (Liu et al., 2013). The cardioprotective benefits likely result from FGF21 activating phosphatidylinositol 3-kinase/Akt, ERK1/2 and

AMPK. Inhibition of these pathways causes a significant reduction of the cardioprotective effect in cardiac ischemia (Patel et al., 2014).

A recent work from Planavila and colleagues has demonstrated that FGF21 knock-out mice develop an increased heart weight and show more signs of dilatation and cardiac dysfunction after isoproterenol injections. Furthermore, these mice showed an increase in cardiac hypertrophy markers such as atrial natriuretic factor (ANF) and α-skeletal actin (α-SKA), as well as pro-inflammatory markers such as interleukin-6 (IL-6) and monocyte chemoattractant protein-1 (MCP-1). Interestingly, treatment with FGF21 could reverse these effects (Planavila et al., 2013). In cardiac remodeling, FGF21 seems to play a role in reducing cardiac hypertrophy by the activation of the MAPK cascade with the help of FGF21/FGFR1 and KLB signaling (Itoh and Ohta, 2013). Because of the involvement of oxidative stress in the etiology of heart disease researchers started to focus on reactive oxygen species (ROS). FGF21 regulates genes that exhibit antioxidant properties (Gomez-Samano et al., 2017). In Sirt-1 knock-out mice this antioxidative effect was markedly reduced, which leads to the conclusion that the expression of *FGF21* is Sirt-1 related (Planavila et al., 2013). Despite the fact that FGF21 is mainly secreted in the liver and acts through an endocrine mechanism, cardiomyocytes are also able to produce FGF21 under oxidative stress condition, and therefore, cardiac FGF21 acts in an autocrine or paracrine manner (Di Lisa and Itoh, 2015).

1.3. Therapeutic potential of fibroblast growth factor 21

1.3.1. Liver

Because of the various beneficial effects of FGF21 on the metabolism, FGF21 has promising potential to cause positive effects on various liver diseases, especially those with a metabolic pathogenesis such as metabolic dysfunction-associated steatotic liver disease (MASLD). The liver is a vital heterogenous organ that has several physiological functions in macronutrient metabolism, immune system, blood volume regulation, endocrine mechanisms, lipid and cholesterol homeostasis and degradation of xenobiotics and toxins (Trefts et al., 2017). MASLD is one of the most common causes of chronic liver disease worldwide and is defined as hepatic

steatosis, histologically at least 5%, without secondary causes such as alcohol abuse, and without signs for hepatocellular injury or steatosis, whereas metabolic dysfunction-associated steatohepatitis (MASH) is described as the presence of at least 5% steatosis and inflammation (Kanwal et al., 2021). MASLD can result in MASH over time, which is associated with a higher risk of cardiovascular disease and liver- and cardiovascular-related mortality. Patients with MASH can develop liver cirrhosis, liver failure and even hepatocellular cancer (HCC). MASH is therefore a very serious disease (Kanwal et al., 2021).

The pathogenesis of MASLD is still not completely understood but insulin resistance, lipid metabolism and inflammation have already been described as important causes for the disorder (Falamarzi et al., 2022). A trial from Rusli and colleagues has discovered higher FGF21 levels in patients with MASLD, prompting claims that FGF21 could be used as a prognostic marker for diagnosis and prediction of liver fat accumulation and dysregulation of metabolic pathways (Rusli et al., 2016). A trial from 2016 confirmed that FGF21 can improve insulin resistance, one of the main causes for MASLD. In an experiment with Monosodium L-glutamate (MSG)-induced obese mice receiving FGF21 an improvement in abnormal glucose tolerance and hyperinsulinemia was observed (Zhu et al., 2016). FGF21 is also able to regulate oxidative stress, ER stress, inflammation and mitochondrial dysfunction in order to decelerate MASLD progression (Ke et al., 2019). In DIO mice Keinicke and colleagues have shown that subcutaneous administration of FGF21 reduced hepatic inflammation and fibrosis (Keinicke et al., 2020).

To use FGF21 as a potential drug, analogues needed to be developed due to the the short half-life of 0.5 to 2 hours, poor stability and bioavailability (Zarei et al., 2020). Pegbelfermin (BMS-986036) is a PEGylated human FGF21 analogue that was tested in a multicenter, randomized, double-blind, placebo-controlled, parallel-group, phase 2a study (Sanyal et al., 2019). Sanyal and colleagues treated overweight or obese patients with non-alcoholic steatohepatitis with subcutaneously administered pegbelfermin for 16 weeks and were thereby able to significantly reduce the liver fat fraction in patients with MASH.

Another analogue called efruxifermin, a long-acting Fc-FGF21 fusion protein, was tested in a randomized, double-blind, placebo-controlled, phase 2a trial on patients with MASH (Harrison et al., 2021). The treatment led to a statistically significant reduction of the hepatic fat fraction, liver stress and injury markers in patients, with mainly gastrointestinal tolerable side effects. Additionally, it reduced triglycerides, LDL, fasting glucose and insulin. It elevated adiponectin levels and HDL and could even ameliorate glycemic control (Harrison et al., 2021).

In a multicenter, double-blind, parallel design trial with obese study participants with mildly hypertriglyceridemia, LLF580, a different genetically synthesized variant of FGF21, was able to reduce liver fat and LDL levels and improve serum lipid levels, liver function and biomarkers for liver injury (Rader et al., 2022).
Not only MASLD and MASH are conditions of interest: there are recent studies regarding alcoholic fatty liver disease and HCC with promising outcomes for the therapeutic potential of FGF21 (Falamarzi et al., 2022).

1.3.2. Diabetes and obesity

Previous preclinical studies have already investigated the promising effects of FGF21 on metabolic mechanisms that are important for the pathogenesis of diabetes and obesity. In a trial from Xu and colleagues the insulin sensitizing and glucose lowering effect of FGF21 has been demonstrated. In ob/ob mice injections with FGF21 resulted in reduction of glucose and insulin levels. Besides that, in DIO mice FGF21 treatment improved glucose tolerance and insulin sensitivity (Xu et al., 2009b). A large number of biopharmaceutical strategies have already been tested in clinical trials. In a randomized, placebo-controlled, double-blind proof-of-concept trial from Gaich and colleagues the FGF21 analogue LY2405319 (LY) was tested on obese patients with type 2 diabetes. The drug improved dyslipidemia, body weight, fasting insulin and adiponectin in humans without a significant decrease of glucose levels (Gaich et al., 2013). Moreover, the long-acting FGF21 analog PF-05231023 ameliorated body weight, dyslipidemia and adiponectin levels, and changed bone resorption and formation parameters in obese patients with type 2 diabetes but again, while not improving glycemic control (Talukdar et al., 2016).

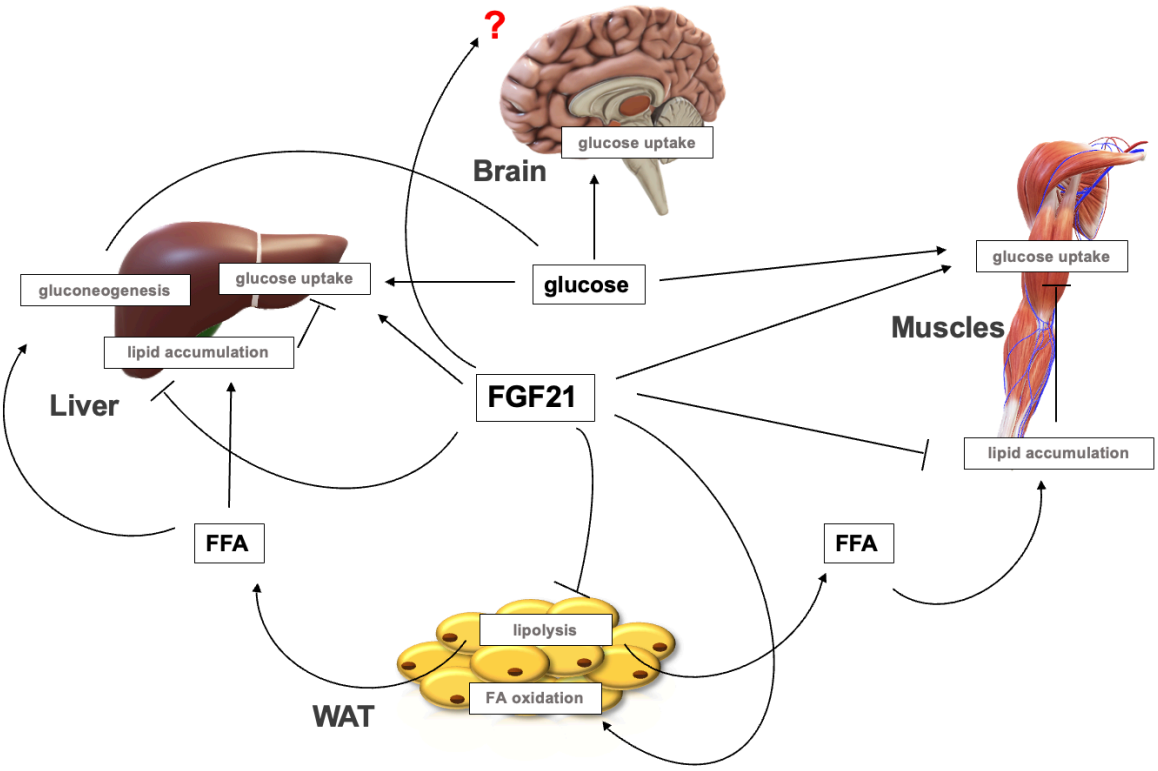

Figure 2: FGF21 in metabolic disease
adapted from (She et al., 2022)

1.3.3. Issues regarding therapeutic targets

As previously described, the development of effective FGF21 analogues that can bind to the FGFR1/KLB complex and overcome the challenges of a short half-life, instability and bioavailability, is possible. Despite that, there are some difficulties to discuss in future trials.

Notably, there is some inconsistency in the effect of FGF21 under physiological conditions compared to the treatment with FGF21 in pharmacologically higher doses. Secreted FGF21 from hepatocytes can induce gluconeogenesis, whereas intracerebroventricular treatment with FGF21 in fasted FGF21-KO mice results in a reversed hypoglycemic effect (Liang et al., 2014). Moreover, subcutaneous injections with FGF21 reduce hypoglycemia, hypolipidemia and insulin resistance in rodents (Xu et al., 2009b). Further trials are required to improve the understanding of this paradox.

Next, not all findings in animal models are applicable in clinical trials on the human species. Growth hormone cannot regulate *FGF21* expression in humans as it does in mice (Geng et al., 2020). Besides, the expression of *KLB* varies significantly between mice and humans. In humans, *KLB* is highly expressed in adipose tissues, liver, pancreas, breast and bone marrow, whilst in mice, evidence for high expression of *KLB* was observed in liver, hypothalamus, pancreas, gall bladder and colon (Geng et al., 2020).

Another notable point is the possible resistance of FGF21 in obesity. In a study from 2010, Fisher and colleagues measured elevated FGF21 plasma levels in DIO mice with a poor response to exogenous administration of FGF21 (Fisher et al., 2010). Berglund et al. examined the effects of acute and chronic FGF21 administration in ob/+ and ob/ob mice. Notably, all investigated effects such as improvement of insulin sensitivity, suppression of gluconeogenesis, elevation of glycogen and lowering of glucagon are weaker in ob/ob mice compared to ob/+ mice (Berglund et al., 2009). In a previous trial investigating effects of FGF21 in the heart, scientists have observed increased expression of *FGF21* in obese rat hearts in comparison to lean rat hearts. In addition, FGF21 signaling was significantly compromised in hearts of obese mice and the cardioprotective effects were also markedly reduced (Patel et al., 2014).

Finally, a large number of trials have proved the beneficial effects of FGF21 administration with results showing improved lipid plasma levels and less hepatic fat fractions, as well as less ischemic and structural heart dysfunctions in humans for the potential future treatment of metabolic-related disorders. Despite the fact that FGF21 treatment could ameliorate insulin sensitivity, it could not improve glycemic control in most of the present trials. Further investigations with longer duration time and larger participant numbers are needed to evaluate clinical efficacy and safety for FGF21-based pharmacotherapies (Geng et al., 2020).

1.4. Organ explant culture

For the investigation of further effects of FGF21 on metabolism and cell signaling, different methods can be applied. The use of cell cultures and animal experiments with mice and other rodents are already well established. As an alternative, in this diploma thesis organ explants, specifically from gonadal and inguinal white or brown adipose tissues from mice, were used for the experiments that will be described in this work.

There is existing literature on organ explants, used to answer various questions in research. Already in the year 1991, Resau and colleagues reviewed the benefits of organ explant cultures (Resau et al., 1991). They defined organ culture or explant culture as whole organs or segments of organs from animals that are *in vitro* cultured in special media. The method distinguishes from cell culture in the composition of culture, as organ culture contains a large amount of different cell types, whereas cell culture consists of a homogenous isolation of defined cells (Resau et al., 1991). The most important benefit of organ cultures lies in the fact that there are intact relations between different cell types. Communication and architecture of the cell complex are still preserved, and the culture reflects a more realistic model of an animal or human organism than standard cell culture could imitate. A prior review from Schweiger and colleagues working on the measurement of lipolysis has taken a closer look at different methods and described a technique, by using organ explants from WAT to measure basal and stimulated lipolysis from tissue depots (Schweiger et al., 2014). The reported protocol for organ explants was used as model for the experimental methods of this work.

1.5. Aim of the study

Previous studies investigated effects and signaling pathways of FGF21 and its metabolic impact almost exclusively in cell culture and animal experiments. Although research has illuminated a variety of effects regarding FGF21 on metabolism in liver and adipose tissue, no study to date has examined those effects in organ explant culture.

This diploma thesis was designed to test the performance of a newly developed modified murine FGF21 in cell culture *(i)* and murine adipose tissue primed *in vivo* before use *ex vivo (ii)*. Furthermore, the work assessed if organ explant culture can be utilized to demonstrate effects of FGF21 and other receptor mediated signaling pathways *(iii).* The work should explore if transmembrane receptors required for FGF21 signaling are still present on the cell surface and allow for signaling of FGF21 by phosphorylation of ERK as a well-known signaling pathway. In conclusion, the prior technique was studied to be used in future research to gain new insights in FGF21 signaling and its impact on metabolism.

2. MATERIAL & METHODS

2.1. Materials

DEVICE	PRODUCER
Centrifuge Heraeus™ Fresco 17	Thermo Scientific™
ChemiDoc™ Touch Imaging System	Bio Rad
LightCycler® 480 System	Roche
MagnaLyser	Thermo Scientific™
My Cycler® Thermal Cycler	Bio Rad
NanoDrop™ 2000	Thermo Scientific
PowerPac 3000	Bio Rad
SPECTROstar® Omega	BMG Labtech

Table 1: *Devices*

MATERIAL	PRODUCER
0.1M DTT	Invitrogen
5x First Strand Buffer	Invitrogen
Acrylamid 30% Acrylamide/Bis Solution	Bio Rad
Aqua bidest. „Fresenius“	Fresenius Kabi Austria GmbH
BCA Protein Assay Kit	Thermo Scientific
β -Mercaptoethanol	Sigma Aldrich MERCK Entellan New
Bromphenol blue	MERCK
Chloroform	EMPLURA
Clarity Western ECL Substrate	Bio Rad
dNTP: Polymerisation Mix	GE Healthcare life Science
EDTA	Sigma
Ethanol	EMPLURA
hFGF21 #2539-FG	R&D Systems
FGF19 #969-FG	R&D Systems
Glycerol	MERCK
Glycin	Millipore

HEPES-KOH	Sigma
Insulin bovine #I6634	Sigma-Aldrich
Isopropanol	EMPLURA
MagNA Lyser Green Beads	Roche
Milk powder	Millipore
Mini-PROTEAN® 3 Cell	Bio Rad
NaCl	MERCK
Nitrocellulose membrane	Bio Rad
Ponceau S Solution	Sigma
PPI	Pierce Thermo Scientific
Precision Plus Protein Dual Color Standards	Bio Rad
Random Hexamer	Applied Biosystems™
RNAse Inhibitor	Applied Biosystems™ Thermo Fisher Scientific
Saccharose	ROTH
SDS, Doclecylsulfate-Na-salt in pellets	SERVA
SuperScript™ II Reverse Transcriptase	Invitrogen
SYBRgreen: Luna® Universal qPCR Master Mix	New England Biolabs
TEMED	BioRad
TRIzol™ Reagent	Thermo Fisher Scientific
Tween 20	Merck

Table 2: *Materials*

ANTIBODIES	**NUMBER**	**PRODUCER**
ACLY	#15421-1-AP	Thermo Fisher
KLB	#AF2619	R&D Systems
mFGF21 goat	#16842	Santa cruz
pAkt	#9614	Cell signaling
pAkt Th308	#4056S	Cell signaling

pAMPK	#2535	Cell signaling
pERK1/2	#9101	Cell signaling
pHSL	#4126S	Cell signaling
ps6 240/244	#5364	Cell signaling
Anti-goat	#a27014	Invitrogen
Anti-mouse	#7076S	Cell signaling
Anti-rabbit	#7074S	Cell signaling

Table 3: *Antibodies*

Primers used at this work

Gene	fwd (5'- > 3')	rev (5'- > 3')
mHPRT	TTG CTC GAG ATG TCA TGA AGG A	AGC AGG TCA GCA AGG AAC TTA TAG
mEgr1	TAT GAG CAC CTG ACC ACA GAG (21mer)	GCT GGG ATA ACT CGT CTC CA (20mer)
mUXT	CTC ACA GAG CTC AGC GAC AGC	AAA TTC TGC AGG CCT TGT AGT TCT C

Table 4: *Primers*

2.1.1. Generation of a modified murine FGF21

Amino sequence of the modified murine FGF21 (modFGF21) produced in yeast cells (Pichia Pastoris):

MEWMRSRVGTLGLWVRLLLAVFLLGVYQAYPIPDSSPLLQFGGQVRQRYLYTD
DDQDTEAHLEIREDGTVVGAAHRSPESLLELKALKPGVIQILGVKASRFLCQQPD
GALYGSPHFDPEACSFRELLLEDGYNVYQSEAHGLPLRLPQKDSPNQDATSWG
PVRFLPMPGLLHEPQDQAGFLPPEPPDVGSSDPLSMVEPLQGRSPSYAS

*orange: 5 deleted amino acids related to HPIP deletion in hFGF21

* green: mutations

Leu118Cys–Ala134Cys, Ser167Ala, ΔHPIP (= putative FAP and DPPIV cleavage sites)

RESIDUE COUNTING ON MATURE PEPTIDE (i.e. L118 is L146, A134 is A162 and S167 is S195 in entire polypeptide count)

The decision to delete the 5 amino acids was based on the knowledge that ΔHPIP in human FGF21 (hFGF21) is fully biologically active. Mutations were added to improve biostability (Yie et al., 2009).

Used stocks of different purified modFGF21 batches: A5, B1, B3, B4, B6 with/ without signal peptide and different purity (c = 100 ng/mL)

2.2. Cell culture

HUH7 cells were used for the cell culture experiments. The cells were maintained in Dulbecco's modified Eagle medium (DMEM - 4.5 g/L glucose) supplemented with 10% fetal bovine serum (FBS) and 1% penicillin/ streptomycin and cultured at 5% CO2 at 37 °C in a CO2 incubator (Binder CB 170). For subculture, cells were rinsed with phosphate-buffered saline (PBS) to remove media containing FBS. Next, cells were detached by trypsinization using trypsin-EDTA. For a quicker detachment cells were incubated and then aspirated with gentle pipetting to resuspend cells. A tenth of the cell suspension was added to a new flask containing media (1:20) and incubated again. The media was renewed 2 to 3 times a week according to media pH and cell confluency. Cells were treated when confluent and incubated at 37 °C in a CO2 incubator.

2.3. Protein isolation

For protein isolation, the cells were scraped gently from the plates and transferred into Eppendorf tubes containing 250 µL homogenization buffer. The tubes were vortexed and spun down. To break the cell membranes apart the cells were sonicated at 80 Hz for 4 seconds and then centrifugated for 2 minutes at 4°C and 6000 rpm. To minimize contamination the supernatant without pellets was collected in new Eppendorf tubes.

Samples of white adipose tissue from mice were added in MagNA Lyser tubes prefilled with homogenization buffer and magnalyzed at 6500 rpm for 20 seconds. Samples were then centrifuged for 2 minutes at 4°C at 13000 rpm. After that, the supernatant without pellets was collected in new tubes.

Homogenization buffer

For preparation of homogenization buffer, 42.8 g saccharose was dissolved in 400 mL of distilled H20 (dH20). 5 mL HEPES-KOH (pH = 7.5) and 1 mL 0.5M EDTA were added and the solution was filled up to 500 mL with dH20.

2.3.1. Protein measurement

Pierce™ BCA Protein Assay Kit was used for all proteins in the mentioned experiments.

Sample dilutions were made (dilution 1:5) using 5 µL sample solution and 20 µL homogenization buffer per microplate well. To prepare the diluted albumin (BSA) standards the following standard curve was used:

Standard (S)	dilution	preparation	concentration
A	1:2	60 µL homogenization buffer (HB) + 60 µL BSA (c = 2 µg/mL)	1000 ng/mL
B	1:4	60 µL HB + 60 µL of standard A	500 ng/mL
C	1:8	60 µL HB + 60 µL of standard B	250 ng/mL
D	1:16	60 µL HB + 60 µL of standard C	125 ng/mL
Blank	1: ∞	Only HB = blank	0 ng/mL

Table 5: *Preparation of standards for protein isolation*

After preparing the dilutions a 96-well plate was used for pipetting using the following scheme:

	1	2	3	4	5	6	7	8	9	10	11	12
A	**SA**	**SA**	**Sample4**	**Sample4**								
B	**SB**	**SB**	**Sample5**	**Sample5**								
C	**SC**	**SC**	**Sample6**	**Sample6**								
D	**SD**	**SD**	**…**	**…**								
E	**Blank**	**Blank**										
F	**Sample1**	**Sample1**										
G	**Sample2**	**Sample2**										
H	**Sample3**	**Sample3**										

Table 6: *Pipetting scheme for protein measurement*

Each well contained 25 µL of the needed dilutions. In the next step working reagent (WR) was prepared by mixing 50 parts of BCA Reagent A with 1 part of BCA Reagent B (50:1, Reagent A:B) from the Pierce™ BCA Protein Assay Kit. 200 µL of WR was pipetted quickly in each well, then the microplate was incubated for 30 minutes at 37°C. To measure the absorbance of the samples a spectrophotometer (SPECTROstar Omega) set to 562 nm was used. After blank-correction of the measurements, the protein concentrations were extrapolated with the help of the standard curve and the formula y = ax + c.

2.4. Western Blot

Preparation of materials

10% Aminopersulfat (APS) = 1 g APS in 10 mL dH20, stored at -20°C

Running buffer (10X):

10X Running buffer: 60 g Tris + 288 g glycine + 20 g SDS filled up to 2 L with dH20

3X SDS sample buffer:

188 mM TRIS-Cl (pH 6.8)

3% SDS

30% glycerol

0.01% bromophenol blue

Transfer Buffer:

2.8 g TRIS dissolved in 400 mL dH20

14.3 g glycine in 400 mL dH20

Mix together and add 200 mL methanol

Place everything covered on ice (exothermic reaction)

TRIS-buffered saline (TBS) Buffer:

24.2 g TRIS Base (20 mM)

80 g NaCl (137 mM)

Filled up with dH20 to 900 mL

pH was set to 7.6 using HCL

Filled up to 1 L with dH20

100 mL of the stock were diluted with 900 mL dH20

TBS-Tween (TBS-T):

1 mL of Tween was added to 1 L of TBS Buffer

5% milk:

25 g milk powder dissolved in 500 mL TBS-T

1st antibody solution (see Table 9):

Dilution 1:1000 in 5% milk

2nd antibody solution:

Dilution 1:3000 in TBS-T

Preparation of polyacrylamide gels

For the 10% separation gel, 3.34 mL dH20 was mixed with 2.66 mL of 30% acrylamide stock and 2 mL separation gel stock. After that, 25 µL 10% ammonium persulfate (APS) and 10 µL tetramethylethylenediamine (TEMED) were added and mixed gently without producing bubbles. For the 4.5% stacking gel 3 mL of dH20 was mixed with 0.75 mL of 30% acrylamide stock and 2 mL collecting gel stock. Next, 10 µL 10% APS and 7.5 µL TEMED were added and mixed gently without producing bubbles. A gel comb was used to form sample loading cells on stacking gel.

Preparation of samples (volume = 20 µL)

Calculated sample volume which was needed for 20 g protein
6.67 µL 3X sample buffer containing 15% β-mercaptoethanol
Filled up with dH20 to 20 µL and cooked at 95°C for 5 minutes

SDS-Page

Clean plastic electrophoresis chambers (Mini-Protean 3 cells from BIORAD) containing gels in corresponding gel holders were filled with 900 mL running buffer. After that, the gel combs were removed, and all samples were load into the gel lanes starting with the pre-stained protein standard (BIORAD) for the protein ladder. The chambers were covered, and anode and cathode were firmly connected. The voltage was set up to 200 V for 10 minutes until the proteins form a straight line. After that, voltage was reduced to 100 V and gel electrophoresis ran for 1.5 hours.

Protein Transfer

In the next step the chambers were opened, and the gels were carefully transferred into a plastic tray filled with transfer buffer. Nitrocellulose membrane, filter paper and sponge support pads were soaked in transfer buffer and the clean plastic chamber containing the transfer tank was filled up with transfer buffer. The plastic cassettes were prepared in the following order starting from the cathode plate of the cassette: sponge, 2x filter paper, gel, nitrocellulose membrane, 2x filter paper, sponge. The cassette was closed by placing the anode plate on top and then carefully placed into the transfer tank. The assembled apparatus was connected with the electrophoresis

power supply and the transfer ran for approximately 1.5 hours at a constant current of 100 V.

Visualization with Ponceau S

After transfer, membranes were removed from the cassettes and placed in Ponceau S for 1 minute. Membranes were then de-stained in dH20 two times. Pictures were taken using ChemiDoc Imager from BIORAD.

Blocking and incubation with 1st antibody

Membranes were placed in 5% milk for one hour until Ponceau S was washed out. After blocking, membranes were incubated in 1st antibody solution (dilution 1:1000 in 5% milk) overnight at 4°C.

Incubation with 2nd antibody

On the next day the membranes were washed in TBS-T 3 times for 15 minutes and then incubated with the 2nd antibody (dilution 1:3000 in TBS-T) for 1 hour at room temperature. After that, membranes were washed out again in TBS-T 3x for 15 minutes.

Visualization on ChemiDoc:

Before visualization, Clarity™ Western ECL Substrate from BIORAD was applied to the membrane for one minute to visualize the horseradish peroxidase-conjugated rabbit anti-mouse immunoglobulins (1:1 Peroxide Reagent to Luminol/Enhancer Reagent). Exposure settings for chemiluminescent imaging were used to acquire the images.

2.5. PCR

Real-time quantitative polymerase chain reaction was performed to detect and quantify the amount of ribonucleic acid (RNA) of the genes of interest. In the first step total RNA was transcribed into complementary DNA (cDNA). After that step cDNA worked as a template for RT-qPCR.

2.5.1. RNA isolation

From adipose tissue:

800 µL TRIzol™ reagent was added in MagNA Lyser tubes prefilled with 50% of ceramic beats. Extracted adipose tissue pieces were added to the tubes and magnalyzed two times at 6500 rpm for 20 seconds. Between steps, samples were cooled down for 2 minutes on ice. Samples were then centrifuged for 3 minutes at 4°C at 13000 rpm. After that, the upper fat layer was removed gently with a pipette and 120 µL chloroform (1:5) was added to each tube, after which they were centrifuged again for 20 minutes.

From cells:

Cells were washed using 1mL PBS. Next, 500 µL of TRIzol™ Reagent was added to each well to lyse the cells. In the next step the lysate was pipetted up and down several times in order to homogenize. The lysate was transferred to a new tube on ice. 100 µL chloroform was added to the tubes and mixed gently for 15 seconds. Samples were centrifuged for 25 minutes at 4°C at 13000 rpm to separate the mixture into three layers: a lower red chloroform phase, a white interphase containing precipitated DNA, and a colorless upper aqueous phase containing the RNA.

The aqueous upper phase was carefully removed using a pipette and transferred into a new Eppendorf tube. 200µL isopropanol was then added, mixed gently with the sample and left on ice for 30 minutes. Samples were centrifuged at 4°C for 25 minutes at 13000 rpm until pellets were formed at the base of each tube. The isopropanol was carefully removed. For the washing step, 500 µL 70% Ethanol on room temperature was added to the pellet, the samples were vortexed and centrifuged for 5 minutes, then the washing step was repeated. The supernatant was removed, and the pellet was dried at room temperature for 10 minutes until it became transparent again. Next, dH20 was added to the tube to dissolve the pellet. The tubes were then heated up for 10 minutes at 60°C and after that, they were left on ice for one hour. For the last step, RNA concentration was evaluated on a NanoDrop™ 2000 spectrophotometer by measuring the absorbance at 260 nm (260/280 ratio should be around 2). Samples were diluted to the desired

concentration, using dH20. The isolated RNA should be stored at –80°C with minimal freeze-thaw cycles.

2.5.2. cDNA synthesis

For the quantification of the gene expression, the qPCR method requires DNA. Therefore, cDNA synthesis is needed for the process to create complementary DNA from an RNA template through reverse transcription. The polymerase reverse transcriptase catalyzes the conversion of RNA into DNA. For this reaction the main components include RNA, buffer, deoxynucleotide triphosphates (dNTP), dithiothreitol (DTT), RNAse inhibitor, primers and nuclease-free water.

Samples were prepared in RNAse-free microfuge tubes by adding 500 ng isolated RNA and using dH20 to fill up the solution to a total volume of 7.5 µL.

Preparation of cDNA Mastermix (total volume 7.5 µL)

dH20	**1.78 µL**
5X First Strand Buffer (Invitrogen™)	3 µL
0.1M DTT (Invitrogen™)	1.5 µL
dNTP (Invitrogen™)	0.22 µL
Superscript II (Invitrogen™)	0.35 µL
RNAse inhibitor (Applied Biosystems™)	0.35 µL
Random hexamer (Thermo Scientific™)	0.3 µL

Table 7: *cDNA Mastermix*

7.5 µL of cDNA Mastermix was added to 7.5 µL of isolated RNA sample. A non-template control containing RNA and cDNA Mastermix components was prepared. All tubes were placed in Thermocycler (MyCycler, BIO-RAD) and PCR ran with the following general settings: 42°C for 90 minutes, 70°C for 15 minutes and 4°C on hold until samples were put on ice.

cDNA dilutions and standard

For the next step, 10 µL of synthesized cDNA was mixed with 190 µL dH20 (1:20 dilution). The leftover cDNA of all samples was collected in an extra tube to create a cDNA pool for the standard curve. The standard curve was pipetted according to the following scheme:

Standard	**cDNA**	**dH20**	**dilution**
S_1	50 µL	200 µL	1:5
S_2	125 µL of S_1	125 µL	1:10
S_3	125 µL of S_2	125 µL	1:20
S_4	125 µL of S_3	125 µL	1:40
S_5	50 µL of S_4	150 µL	1:160

***Table 8**: Preparation of standards for cDNA synthesis*

2.5.3. RT-qPCR

Each investigated gene requires two primers for the next step. The primers were diluted in nuclease free water by mixing 10 µL (= 5 pmol) of forward and 10 µL (= 5 pmol) of reverse primer with 180 µL of nuclease free water in a fresh RNAse-free tube. SYBR Green dye was used for the quantification of the gene expression. The free-floating fluorescent dye can bind to double-stranded DNA molecules and intercalate between the DNA bases, which leads to an increase in fluorescence intensity. The concentration of double-stranded DNA correlates with the fluorescence intensity, which can be measured at the end of each amplification cycle. To create the PCR Mastermix, the diluted primers, nuclease-free water and SYBR Green were mixed together accordingly to the following protocol:

Preparation of PCR Mastermix SYBR Green for duplicates:

SYBR Green qPCR Mastermix	10 µL	Contains SYBR Green dye, DNA polymerase, buffer and stabilizer, dNTPs
Nuclease-free water	5 µL	
Forward primer	0.5 µL	= 1 µL of the diluted primers (5 pmol)
Reverse primer	0.5 µL	
Total volume	16 µL	= volume for one duplicate

Table 9: *PCR Mastermix*

After preparation, 8 µL of PCR Mastermix was added in each well of a 384-well Eppendorf PCR plate using a Multistepper Pipette. Then, 2 µL of cDNA was pipetted into each well. For controls, dH20 was used as negative control and RNA as no template control. At the end of the procedure, the plate was covered with protective foil and centrifuged for 1 minute at 900 rpm. To analyze the amount of transcribed mRNA of the investigated genes, the plate was put in Lifecycler 480 to run the cycle program. mRNA levels were normalized to mRNA of the reference genes *Hprt* and *Uxt*. Relative quantification of double standard curves was used to identify the relative concentration of cDNA.

Pipetting scheme 384-well plate for RT-qPCR

	1	2	3	4	5	6	7	8	9	10	11	12	13	14	15	16	17	18	19	20	21	22	23	24	
A	S1		S2		S3		S4		S5		RNA		H20												
B	K 2 (2)		K 3 (3)		FGF19.1 (4)		FGF19.2 (5)		FGF19.3 (6)		hFGF21.1 (7)		hFGF21.2 (8)		hFGF21.3 (9)		A5.1 (10)		A5.2 (11)		A5.3 (12)		B1.1 (13)		HPRT
C	B1.2 (14)		B1.3 (15)		B3.1 (16)		B3.2 (17)		B3.3 (18)		B4.1 (19)		B4.2 (20)		B4.3 (21)		B6.1 (22)		B6.2 (23)		B6.3 (24)				
D	S1		S2		S3		S4		S5		RNA		H20												
E	K 2 (2)		K 3 (3)		FGF19.1 (4)		FGF19.2 (5)		FGF19.3 (6)		hFGF21.1 (7)		hFGF21.2 (8)		hFGF21.3 (9)		A5.1 (10)		A5.2 (11)		A5.3 (12)		B1.1 (13)		EGR1
F	B1.2 (14)		B1.3 (15)		B3.1 (16)		B3.2 (17)		B3.3 (18)		B4.1 (19)		B4.2 (20)		B4.3 (21)		B6.1 (22)		B6.2 (23)		B6.3 (24)				

Table 10: *Pipetting scheme for qPCR*

2.6. Organ explant culture

Male and female C57BL/6 mice kindly provided from the lab group AG Fickert were used in all experiments, euthanized by cervical dislocation and adipose tissues from different fat pad depots (gonadal and inguinal WAT; BAT) were immediately dissected for further processing. The freshly eviscerated tissue was cut into small 0.5 cm pieces and transferred to 6-well plates containing 400 µL preincubated media at 37°C.

Different sera were tested, to try reducing the amount of protein that might intercalate with the receptors for FGF21 signaling. Therefore, 2% charcoal-stripped fetal bovine serum (FBS), a serum treated with activated carbon to eliminate non-polar/lipophilic components like steroids, growth factors and cytokines, 2% dialyzed FBS containing reduced amounts of small molecules like amino acids, hormones and cytokines were used. In later experiments phosphate-buffered saline (PBS) was tested to determine if missing serum could improve FGF21 signaling.

3. RESULTS

3.1. Modified FGF21s activate ERK signaling in human liver cells

In order to explore if the newly developed modified murine FGF21s (batches used: A5, B1, B3, B4) mediate signal transduction, HUH7 cells were tested for FGF21 signaling. Although this is a human liver cell line, it is well-known that HUH7 cells express FGFR4 and in smaller amounts FGFR1 (Asada et al., 2003). For that reason and for the ready availability of the cell line in the lab, the experiments were started with the hepatocytes. The peptide FGF19 binds to FGFR4 in the liver and similar to the signaling cascade of FGF21 induces phosphorylation of ERK1/2. Thus, FGF19 served in the following experiments as a positive control to verify if the modFGF21s are able to activate the same signaling cascade via binding to the complex of FGFR1/KLB or FGFR4/KLB (Adams et al., 2012b). Therefore, protein levels of phosphorylated ERK1/2 were examined by performing western blot analysis. In cells stimulated with FGF21, the phosphorylation of ERK1/2 implicates that FGF21 can bind to the receptor complex. The pilot experiment demonstrated clearly present protein levels of pERK1/2 regardless of the different treatment times of 30 minutes and 2 hours in the untreated control group, FGF19-, B4- and B5-treated groups. The highest increase was found in the treatment with B4. However, incubation with batches A5 and B1 decreased protein levels of pERK1/2 dramatically. Batch B5 showed a slight elevation of pERK1/2 (Fig. 3).

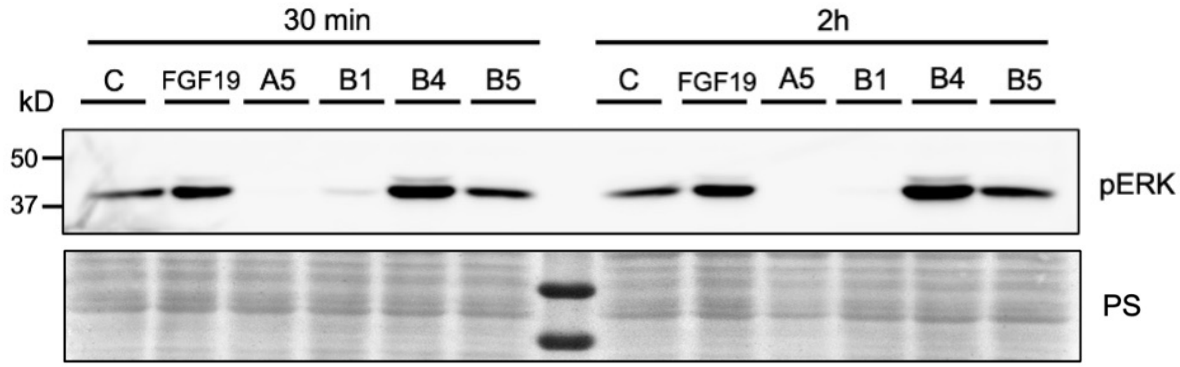

Figure 3: Protein levels of pERK1/2 in HUH7 cells treated with different stocks of modFGF21

C = untreated: HUH7 cells incubated in media; FGF19 = positive control: samples treated with media containing FGF19 (c = 100 ng/mL); A5, B1, B4 and B5: samples treated with media containing different stocks of modFGF21 (c = 100 ng/mL); treatment duration: 30 minutes versus 2 hours; PS: Ponceau; anti-phospho-ERK1/2 (Thr202/Tyr204) was used.

3.2. Modified FGF21s induce *Egr-1* expression in human liver cells

To assess the impact of modFGF21 on gene expression downstream of the ERK1/2 pathway, mRNA levels of one of the best known FGF21 target gene downstream of ERK, *Early growth response-1 (Egr-1),* were quantified by RT-qPCR. HUH7 cells treated with the positive controls FGF19 or hFGF21 showed increased mRNA levels of *Egr-1* by 1.7- and 1.4-fold, respectively. Interestingly, in comparison to untreated liver cells, a 1.5-fold increase of *Egr-1* was detected after treatment with modFGF21 of batch B4, while the other batches decreased *Egr-1* mRNA levels, which seems to be in line with the inhibition of pERK1/2. (Fig. 4). This attempt served as an additional readout for ERK activation, but it did not provide the needed sample size to perform statistical analysis.

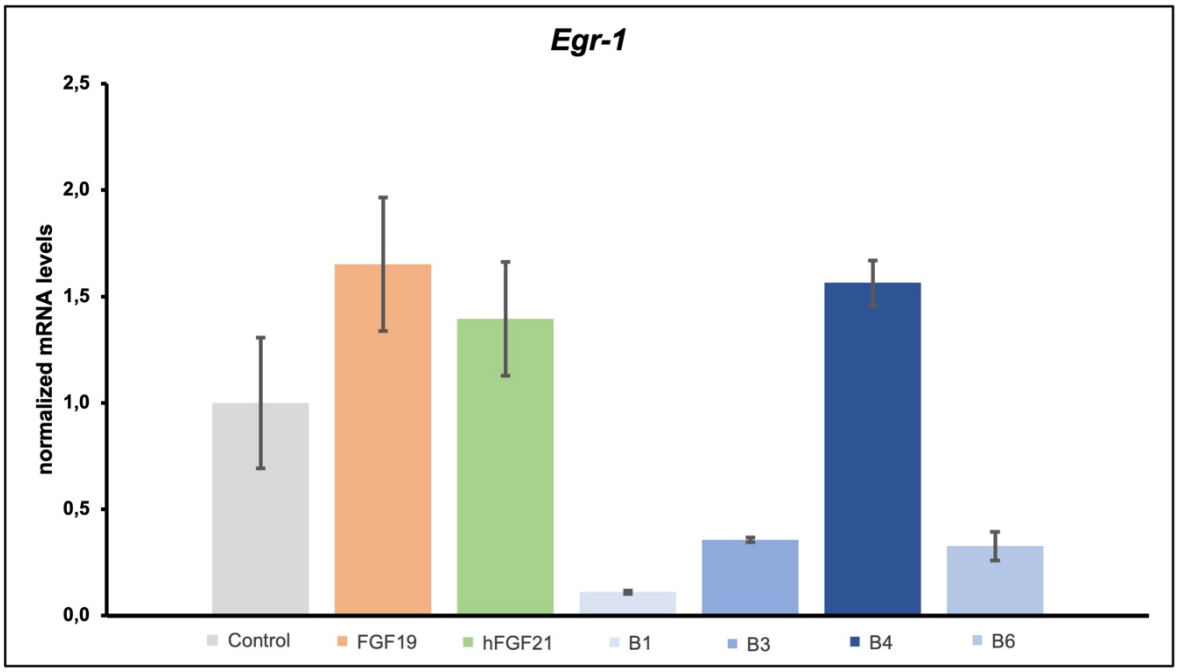

Figure 4: Relative expression of Egr-1 mRNA levels in HUH7 cells
Control: untreated cells; FGF19: cells treated with FGF19 (c = 100 ng/mL), hFGF21: cells treated with recombinant human FGF21; B1, B3, B4, B6 are different stocks of modFGF21 (c = 100 ng/mL); treatment duration: 30 minutes; the results were normalized against hypoxanthine guanine phosphoribosyltransferase (HPRT) and expressed as fold changes in relative mRNA expression. n = 1 in each group. Values represent the mean ± standard deviation (SD).

3.3. FGF21 in white adipose organ explants

3.3.1. Missing induction of FGF21 signaling in organ explants

FGFR1, the receptor with the highest affinity for FGF21 is mainly expressed in WAT. Therefore, adipocytes were needed to test the performance of the newly developed modFGF21 in cell culture.

HUH7 cells represent a realistic model to test FGF19 because of the high expression of FGFR4 on the cell surface of hepatocytes. Nonetheless, FGF21 acts mainly in an endocrine manner on peripheral organs like adipose tissue and it is thus necessary to test modFGF21 in adipocytes. A common way of obtaining adipocytes for cell culture experiments is through the differentiation of pre-adipocytes into mature 3T3L-1 cells, which display different characteristics than mature primary adipocytes. To streamline the procedure and to work with WAT

containing a functional cellular environment of different communicating cell types, the following experiments in this work were realized in surgically removed murine WAT that was placed in a cell culture environment.

To test if the organ explant culture is working in the first experiment, protein levels of pERK1/2 and mRNA levels of its downstream target gene *Egr-1* were quantified. There was no relevant change in protein concentration of pERK1/2 after treating gonadal WAT with modFGF21 (batch B6) compared to purified recombinant hFGF21 or untreated cells. To assess if KLB was still present on the cell surface or internalized after formation of the FGF21/FGFR1/KLB complex, protein levels of KLB were examined. Compared to untreated WAT explants, hFGF21 showed a slight increase of KLB, whereas modFGF21-treated samples showed no difference to control (Fig. 5).

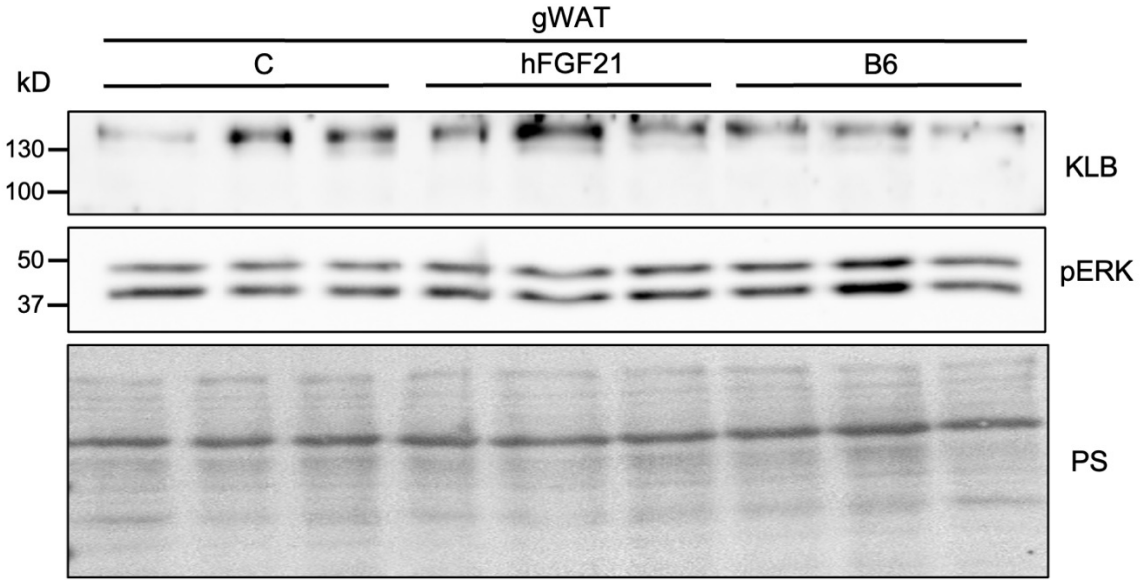

Figure 5: Protein levels of KLB and pERK1/2 in gWAT after treatment
C = Control: cells incubated in media; hFGF21: cells incubated in media containing 10 nM FGF21(c = 200 ng/mL); B3, B4, B6: samples incubated in media containing 10 nM modFGF2 from different stocks (c = 200 ng/mL); treatment duration 30 min; samples incubated in media containing DMEM (4.5 g/L glucose), 10% FBS and 1% penicillin/ streptomycin; anti-phospho-ERK1/2 (Thr202/Tyr204) was used.

Having a closer look at the gene expression levels of *Egr-1* in FGF signaling, adipose tissue treated with modFGF21 B4 and B6 showed a slight increase of *Egr-1* mRNA levels. hFGF21-treated samples showed a 2.1-fold increase of mRNA

levels. In contrast, B3-treated samples decreased *Egr-1* mRNA levels to ~60% compared to untreated control. *Egr-1* mRNA expression served as a second readout. However, the duration of the treatment used to investigate ERK phosphorylation might be not suitable for the measurement of *Egr-1* mRNA expression levels. Therefore, mRNA expression was not investigated in further experiments. The results shown in Figure 6 and 7 did not provide the needed sample size to perform statistical analysis. qPCR results without normalization by the reference gene *Uxt* showed less induction of *Egr-1* through modFGF21s, indicating that this reference gene (housekeeping gene) is impacted by the treatment (Fig. 6-7).

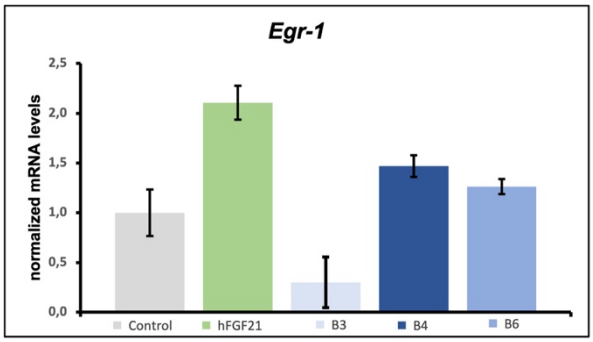

Figure 6: Relative expression of Egr-1 mRNA

(in fold change) in adipose organ explants, results normalized against ubiquitously expressed prefoldin like chaperone gene (Uxt).

Values represent the mean ± SD. n = 1 in each group.

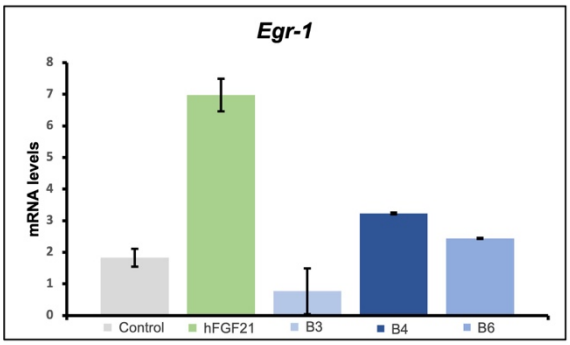

Figure 7: Expression of Egr-1 mRNA

(in ng/µL) in adipose organ explants without normalization to show difference in data without the use of Uxt.

3.3.2. Effects of fasting and refeeding on phosphorylation of ERK1/2 in WAT

To examine if different nutritional status in mice would affect phosphorylation of ERK1/2 in WAT treated with FGF21, the following experiments were performed using WAT from inguinal and gonadal fat depots taken from C57BL mice. With the idea of creating optimal conditions for FGF21 signaling by sensitizing the adipose tissue for the FGF21 treatment, animals were either fasted (14h) or fasted and refed (~4h). After a treatment time of 30 minutes with recombinant human FGF21, samples were processed for protein quantification.

Furthermore, to investigate if the growth factors in FBS might induce the induction of pERK1/2 we compared incubated organ explants with directly processed WAT. Additionally, we lowered the amount of serum in the cell culture media from 10% to 2%.

Organ explant culture using gonadal WAT showed a slightly elevated phosphorylation of ERK1/2 in the incubated ON fasting groups, compared to directly processed control group. Similar elevation of pERK1/2 was found in the preincubated refed group. Samples treated with hFGF21 showed no impact on pERK1/2 in adipose tissue from fasted as well as refed animals compared to the control group in FBS. Overall, organ explants from fasted/refed animals showed slightly higher pERK1/2 levels than explants from only fasted animals (Fig.8).

Organ explant culture using inguinal WAT seems to be more sensitive to ERK activation compared to gWAT, especially in adipose tissue from refed animals. In particular, elevated ERK activation was observed after treatment with hFGF21 in both groups. Only one replicate of the FGF21-treated group could not prove a similar increase. (Fig. 9).

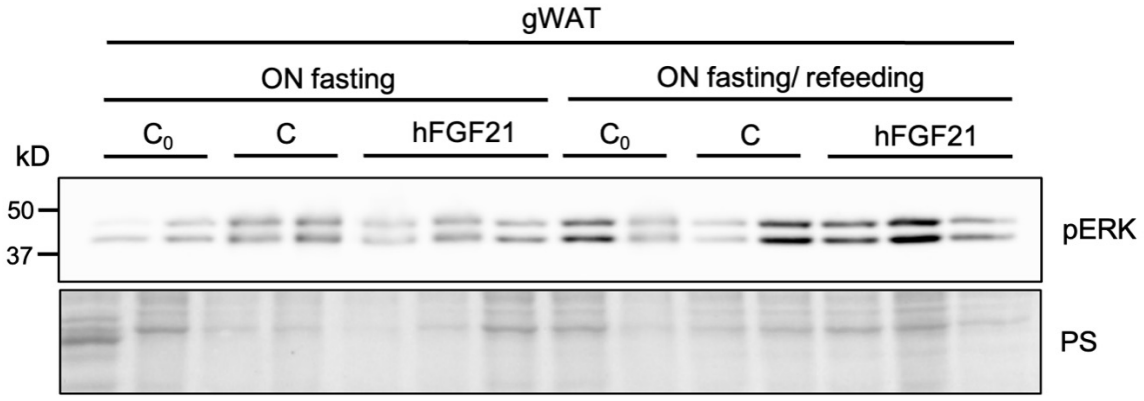

Figure 8: Protein levels of pERK1/2 in gWAT – fasting and refeeding
C_0 = directly processed tissue after resection; C = untreated WAT; hFGF21: samples incubated in media containing hFGF21(c = 250 ng/mL); ON fasting: samples from fasted mice; ON fasting/ refeeding: samples from refed mice (after 4 hours); samples were incubated in media containing DMEM, 2% FBS and 1% penicillin/ streptomycin for 30 minutes at 37°C; PS: Ponceau S.

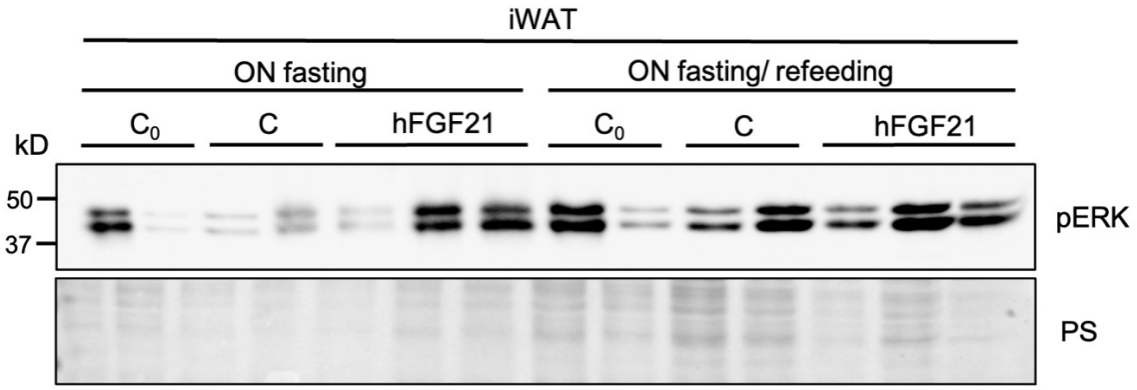

Figure 9: Protein levels of pERK1/2 in iWAT – fasting and refeeding
C_0 = directly processed tissue after resection; C = untreated WAT; hFGF21: samples incubated in media containing hFGF21(c = 250 ng/mL); ON fasting: samples from fasted mice; ON fasting/ refeeding: samples from refed mice (after 4 hours); samples were incubated in media containing DMEM, 2% FBS and 1% penicillin/ streptomycin for 30 minutes at 37°C; PS: Ponceau S.

3.3.3. Signal transduction pathways in organ explants using different FBS

In order to test if common cell signaling generally works in organ explants, samples were treated with insulin or isoproterenol to demonstrate effects on anabolic metabolism and lipolysis in WAT samples. In addition, to exclude negative influences of growth hormones or lipids from FBS we tested the impact of hFGF21, insulin and isoproterenol in dialyzed and charcoal-stripped FBS.

To test the new settings, we incubated gWAT in 2% dialyzed FBS. Next, samples were treated with isoproterenol to activate the β3-adrenergic receptor, insulin to activate the insulin receptor or hFGF21 to activate KLB/FGFR1 and consequently, pERK1/2. As seen in Figure 10, isoproterenol showed a very clear increase of HSL phosphorylation, a downstream target of the β3-adrenergic receptor and cAMP-dependent protein kinase (PKA). However, pERK1/2 was still not activated by hFGF21 in our setting. Interestingly, isoproterenol even decreased pERK1/2 levels, indicating that the ERK pathway is still sensitive to other treatments.

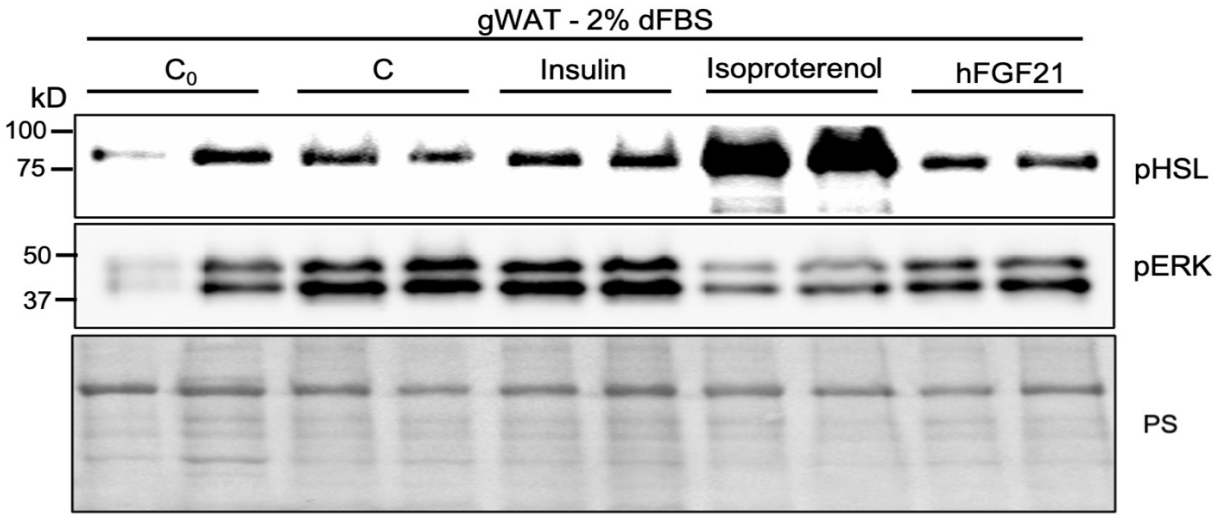

Figure 10: Protein levels of pERK1/2 and pHSL in gWAT – media containing 2% dFBS

C_0 = directly processed tissue after resection; C = untreated WAT; Insulin: samples incubated in media containing 1.72 µM insulin (c = 0.01 mg/mL); Isoproterenol: samples incubated in media containing 0.5 mM isoproterenol (c = 0.1 mg/mL); hFGF21: samples incubated in media containing hFGF21 (c = 500 ng/mL), media containing DMEM with 2% dFBS; treatment duration of 20 minutes; PS: Ponceau S.

In comparison to Fig. 10, the experiment from Fig. 11 shows the data obtained from iWAT. Similar to the last experiment, protein levels of pHSL were increased in samples, treated with isoproterenol. In order to test the regulatory functionality of the anabolic signaling pathway, phosphorylated Akt (pAKT) and ps6 were investigated. Insulin-treated tissue showed elevated pAKT levels, but insulin did not increase ps6 in dialyzed FBS. pERK1/2 levels were not investigated in this experiment.

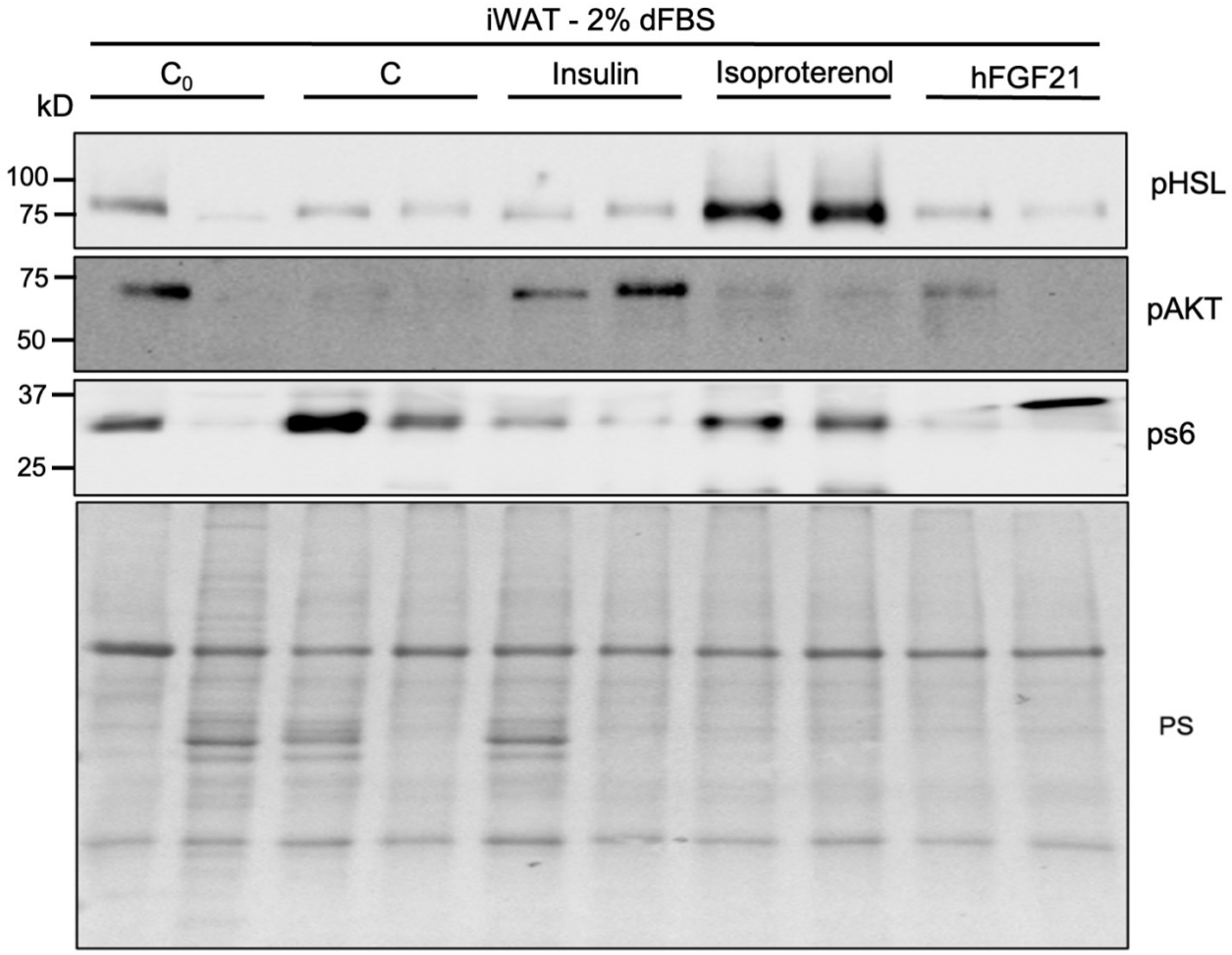

Figure 11: Different protein levels in iWAT – media containing 2% dFBS

C_0 = directly processed tissue after resection; C = untreated WAT; Insulin: samples incubated in media containing 1.72 µM insulin (c = 0.01 mg/mL); Isoproterenol: samples incubated in media containing 0.5 mM isoproterenol (c = 0.1 mg/mL); hFGF21: samples incubated in media containing hFGF21 (c = 500 ng/mL), media containing DMEM with 2% dFBS; treatment duration of 20 minutes; PS: Ponceau S.

In the next experiment, treatments were applied on gWAT incubated in charcoal-stripped FBS (Fig. 12). Increased pHSL levels were found in all groups except from insulin and hFGF21. No clear difference in pERK1/2 levels were observed between hFGF21 and untreated groups. Because of inconclusive results and difficulties in extracting pure proteins, further experiments using csFBS were not conducted, suggesting that cs-FBS might be not suitable for the experimental set-up.

In the following experiment, iWAT was treated with media containing standardized unmodified FBS (Fig. 13). Similar to dFBS, protein levels of pHSL showed the

highest increase in samples treated with isoproterenol. pAKT substrate levels were elevated over all groups incubated in FBS. Treatment with hFGF21 showed no impact on signaling pathways investigated in this setup.

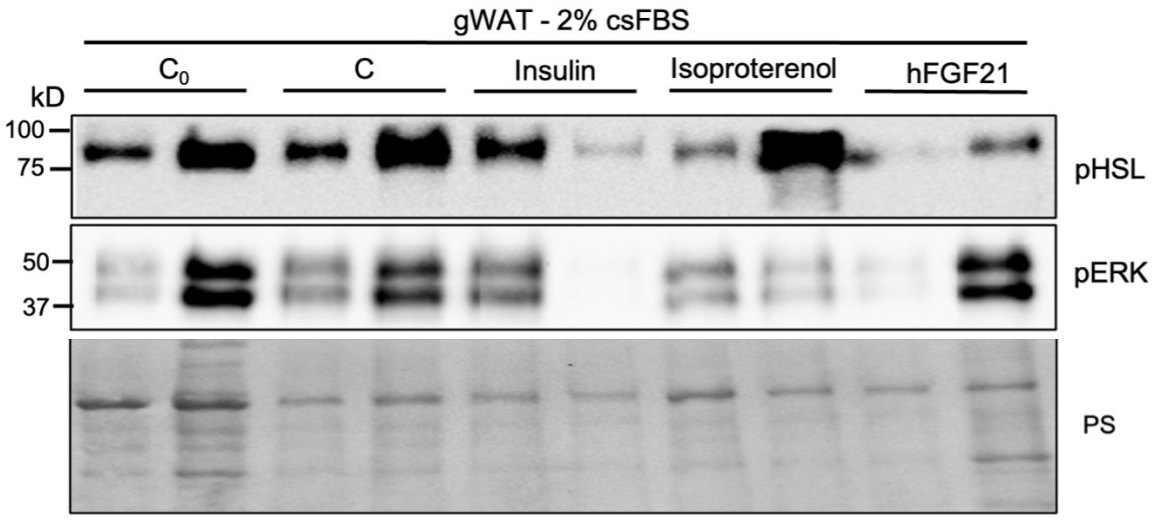

Figure 12: Protein levels of pHSL and pERK1/2 in gWAT – 2% csFBS
C_0 = directly processed tissue after resection; C = untreated WAT; Insulin: samples incubated in media containing 1.72 µM insulin (c = 0.01 mg/mL); Isoproterenol: samples incubated in media containing 0.5 mM isoproterenol (c = 0.1 mg/mL); hFGF21: samples incubated in media containing hFGF21 (c = 500 ng/mL), media containing DMEM with 2% csFBS; treatment duration of 20 minutes; PS: Ponceau S.

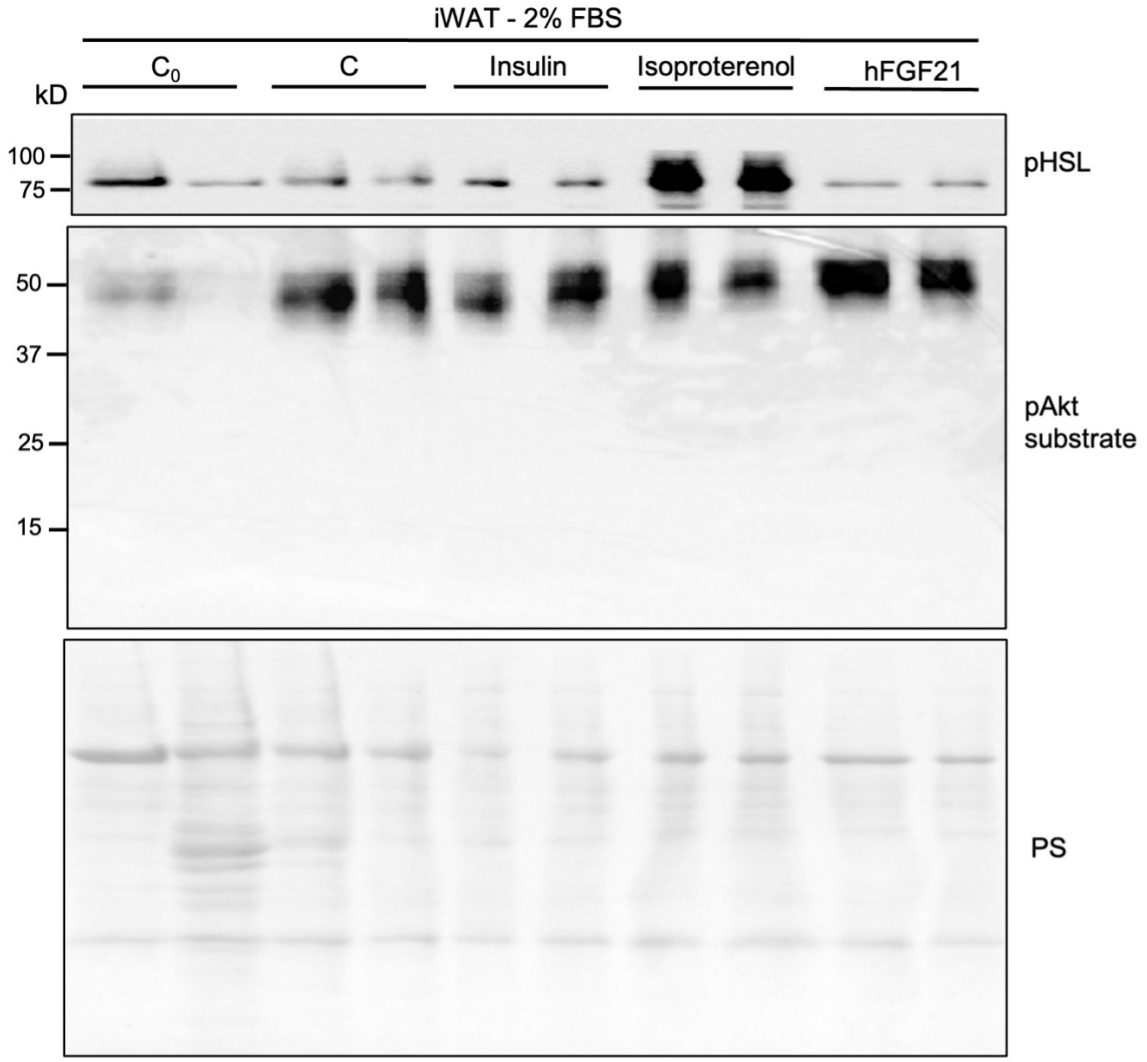

Figure 13: Protein levels of pHSL and pAKT substrate in iWAT – 2% FBS
C_0 = directly processed tissue after resection; C = untreated WAT; Insulin: samples incubated in media containing 1.72 µM insulin (c = 0.01 mg/mL); Isoproterenol: samples incubated in media containing 0.5 mM isoproterenol (c = 0.1 mg/mL); hFGF21: samples incubated in media containing hFGF21 (c = 500 ng/mL), media containing DMEM with 2% FBS; treatment duration of 20 minutes; PS: Ponceau S.

3.3.4. Effects on phosphorylation of proteins in WAT using phosphate-buffered saline

Instead of media containing serum, in the next experimental set-up we did not use FBS but prewarmed PBS to incubate adipose tissue. In gWAT, isoproterenol-treated samples showed an increase in pHSL protein levels and a decrease of ps6. Insulin showed its characteristic elevation of pAKT and ps6, indicating that this setup is suitable and displays consistent results. However, pERK1/2 was only slightly increased in samples treated with hFGF21 (Fig. 14). In iWAT similar results could

be observed, as demonstrated by elevation in protein levels of pHSL, pERK1/2, pAKT and ps6, with hFGF21 showing the least prominent impact of all treatments (Fig. 15).

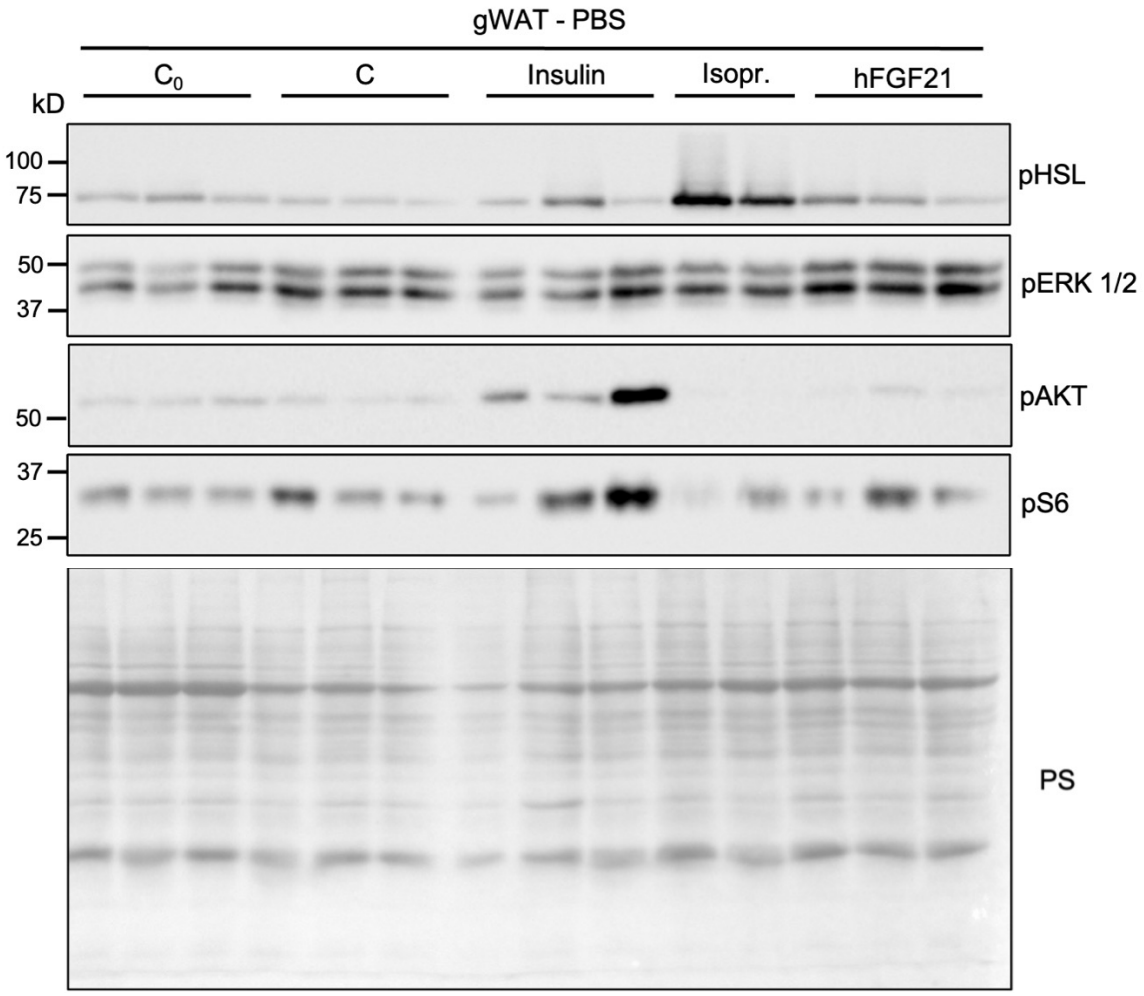

Figure 14: Different protein levels in gWAT – PBS

C_0 = directly processed tissue after resection; C = untreated WAT; Insulin: samples incubated in media containing 1.72 µM insulin (c = 0.01 mg/mL); Isoproterenol: samples incubated in media containing 0.5 mM isoproterenol (c = 0.1 mg/mL); hFGF21: samples incubated in media containing hFGF21 (c = 500 ng/mL), media based on PBS; treatment duration of 20 minutes; PS: Ponceau S.

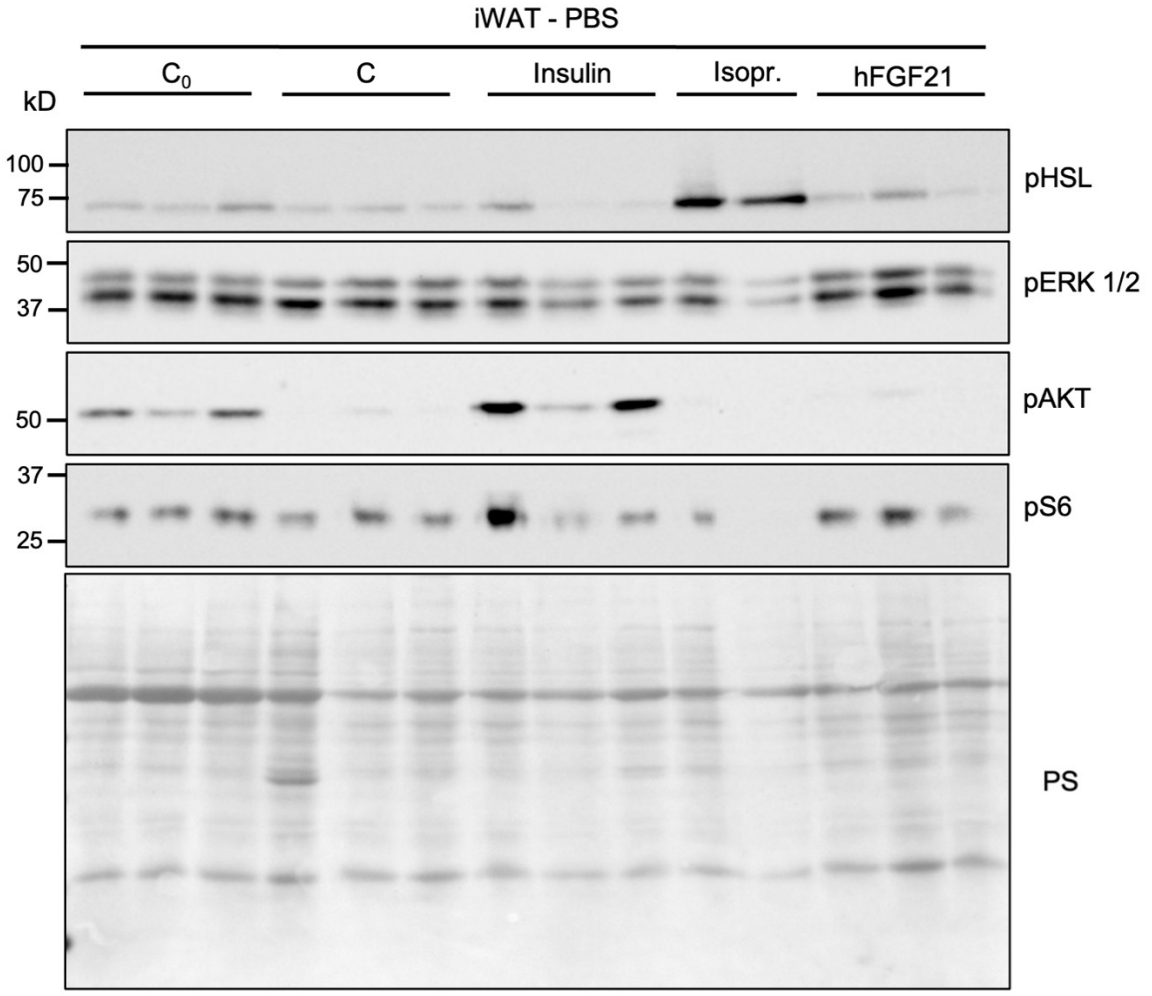

Figure 15: Different protein levels in iWAT – PBS
C_0 = directly processed tissue after resection; C = untreated WAT; Insulin: samples incubated in media containing 1.72 µM insulin (c = 0.01 mg/mL); Isoproterenol: samples incubated in media containing 0.5 mM isoproterenol (c = 0.1 mg/mL); hFGF21: samples incubated in media containing hFGF21 (c = 500 ng/mL), media based on PBS; treatment duration of 20 minutes; PS: Ponceau S.

3.3.5. Preincubation with hFGF21 increases phosphorylation of ERK1/2 levels

For the last experimental set-up gonadal and inguinal WAT was divided into two groups to test the influence of long-term incubation with media before applying different treatments on tissue samples. Group A was preincubated with media for 7.5 hours before treatment for 30 minutes. Group B was preincubated for 7.5 hours as well, but a 2-hour preincubation step with hFGF21 was included after 5.5 hours to explore if explants have to be primed for FGF21.

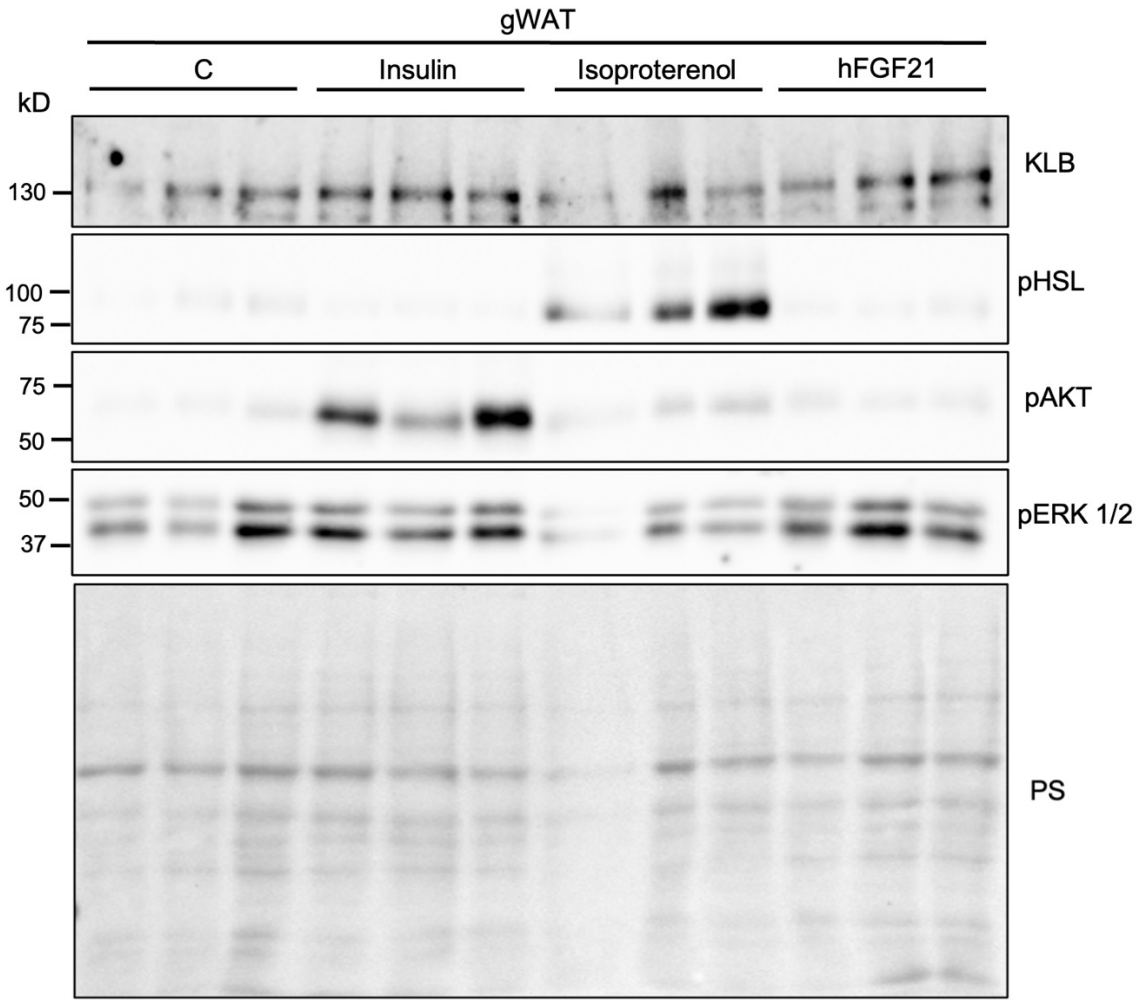

Figure 16: Control group: Different protein levels in gWAT preincubated in media for 8 hours

C =: samples incubated in media; Insulin: samples incubated in media containing 1.72 µM insulin (c = 0.01 mg/mL); Isoproterenol: samples incubated in media containing 0.5 mM isoproterenol (c = 0.1 mg/mL); hFGF21: samples incubated in media containing hFGF21 (c = 500 ng/mL), media containing DMEM, 2% FBS, 1% streptomycin/penicillin; preincubating for 8 hours in media; treatment duration of 30 minutes; PS: Ponceau S.

Data from gonadal WAT (Fig. 16), representing group A, showed that 8h of incubation still allows for an increase in protein levels of pHSL and pAKT, as detected for isoproterenol and insulin, respectively. Moreover, insulin and hFGF21-treated triplicates showed a slightly higher increase in protein levels of pERK1/2. Inguinal WAT incubated with media for 8 hours, representing group A (Fig. 17) showed a comparable induction of pHSL and pAKT levels by isoproterenol and insulin. In almost all groups except for isoproterenol, an elevation of pERK1/2 levels was observed. The highest elevation of protein was found in hFGF21 treated

samples and the lowest protein levels of KLB were observed after treatment with isoproterenol.

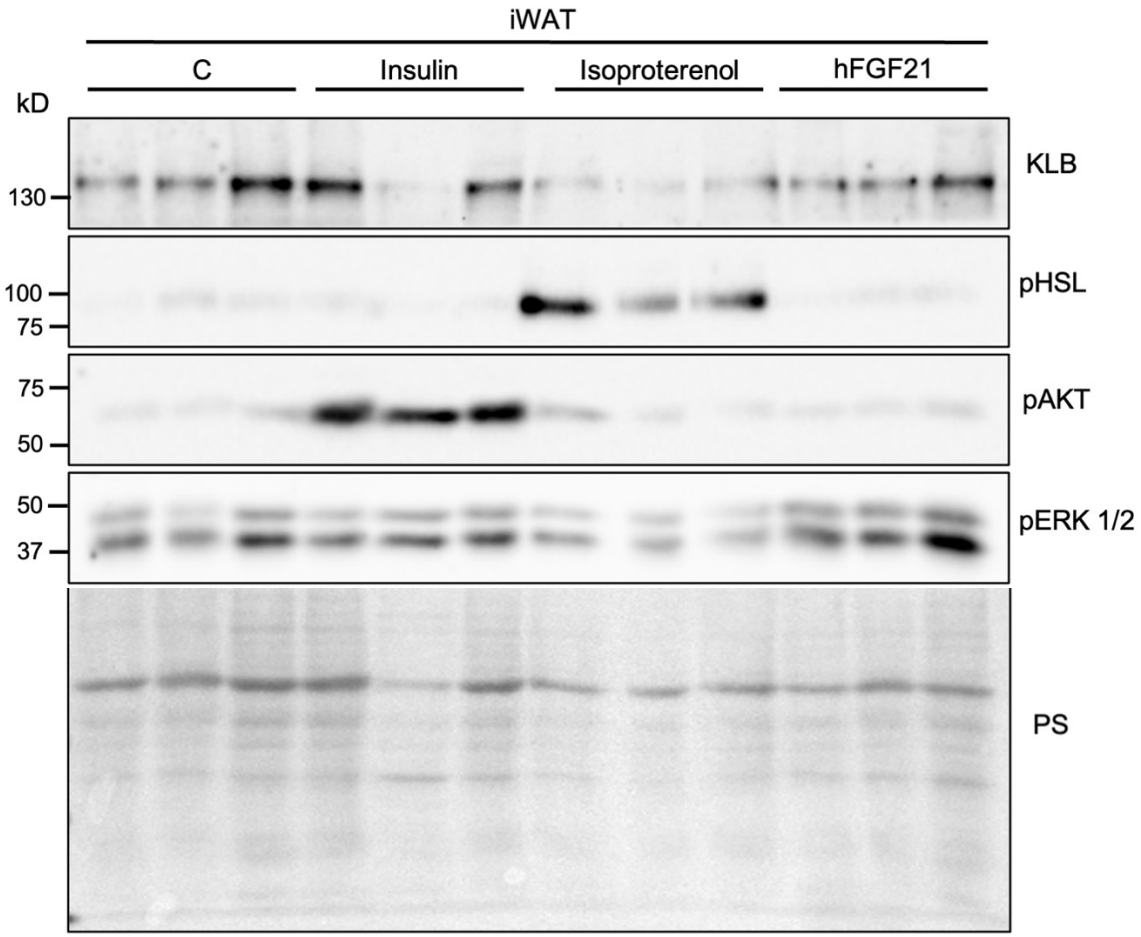

Figure 17: Different protein levels in iWAT preincubated in media for 8 hours
C = samples incubated in media; Insulin: samples incubated in media containing 1.72 µM insulin (c = 0.01 mg/mL); Isoproterenol: samples incubated in media containing 0.5 mM isoproterenol (c = 0.1 mg/mL); hFGF21: samples incubated in media containing hFGF21 (c = 500 ng/mL), media containing DMEM, 2% FBS, 1% streptomycin/penicillin; preincubating for 8 hours in media; treatment duration of 30 minutes; PS: Ponceau S.

In gWAT, preincubation for 2 hours followed by a second high-dose incubation with hFGF21 (Fig. 18) showed similar increase in protein levels of KLB over all western blots. Elevation of pAKT levels were obtained in insulin-treated samples regardless of preincubation with hFGF21, while pERK1/2 levels were not elevated in hFGF21-pretreated groups.

Inguinal WAT was tested in the same manner to explore the effect of preincubation with hFGF21 (Fig. 19-20). Interestingly, in this attempt protein levels of pERK1/2

showed a slight increase towards 5.5/2h-preincubated samples compared to 7.5h preincubation only. Similar protein levels of KLB were observed over all samples and pAKT levels were clearly elevated in insulin-treated samples, similar to previous results (Fig. 19).

Additional results using iWAT showed elevated protein levels of pHSL with a clear decrease of pAMPK and pERK1/2 levels in isoproterenol treated samples. Protein levels of KLB are not consistent. Further, 5.5/2h-preincubated samples in control and hFGF21-treated group showed slightly higher protein levels of pERK1/2 compared to 7.5h preincubation only (Fig. 20).

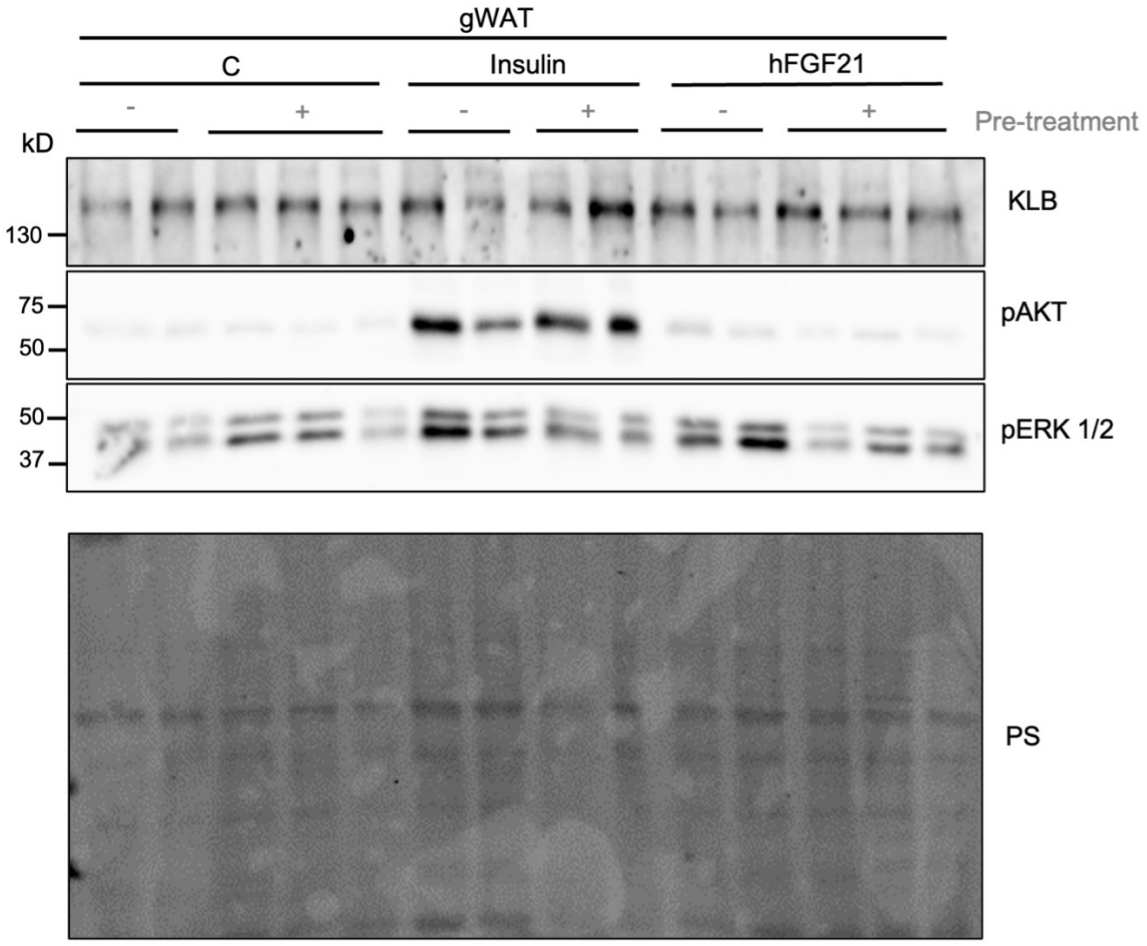

Figure 18: Protein levels of KLB, pAKT and pERK1/2 in gWAT preincubated in media +/- FGF21

C = negative control: samples incubated in media; Insulin: samples incubated in media containing 1.72 µM insulin (c = 0.01 mg/mL); hFGF21: samples incubated in media containing hFGF21 (c = 500 ng/mL), media containing DMEM, 2% FBS, 1% streptomycin/penicillin; preincubating for 8 hours in media; Pre-treatment: samples were (+) or were not (-) preincubated in media containing FGF21 for 2 hours; treatment duration of 30 minutes; PS: Ponceau S.

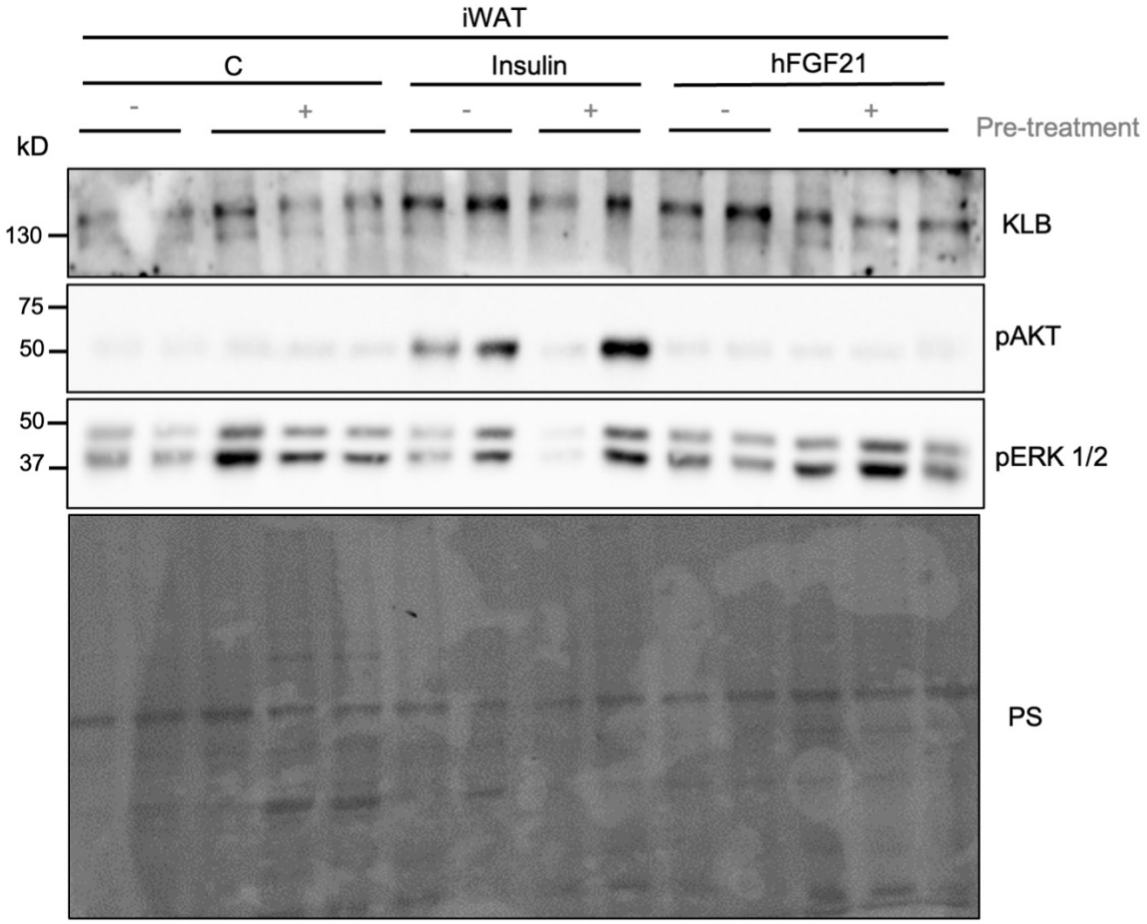

Figure 19: Protein levels of KLB, pAKT and pERK1/2 in iWAT preincubated in media +/- FGF21 for 8 hours

C = negative control: samples incubated in media; Insulin: samples incubated in media containing 1.72 µM insulin (c = 0.01 mg/mL); hFGF21: samples incubated in media containing hFGF21 (c = 500 ng/mL), media containing DMEM, 2% FBS, 1% streptomycin/penicillin; preincubating for 8 hours in media; Pre-treatment: samples were (+) or were not (-) preincubated in media containing FGF21 for 2 hours; treatment duration of 30 minutes; PS: Ponceau S.

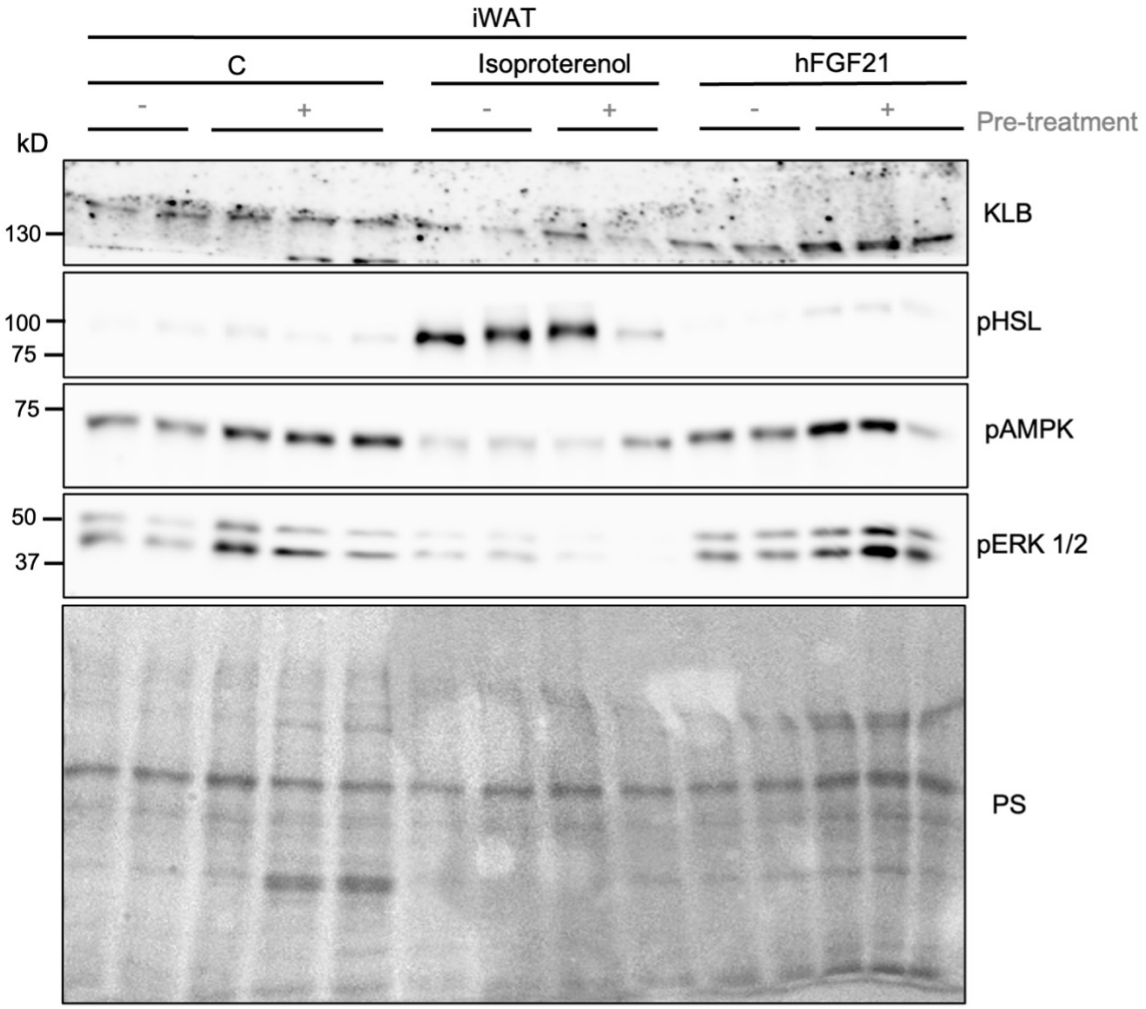

Figure 20: Different protein levels in iWAT preincubated in media +/- FGF21 for 8 hours

C = samples incubated in media; Isoproterenol: samples incubated in media containing 0.5 mM isoproterenol (c = 0.1 mg/mL); hFGF21: samples incubated in media containing hFGF21 (c = 500 ng/mL), media containing DMEM, 2% FBS, 1% streptomycin/penicillin; preincubating for 8 hours in media; Pre-treatment: samples were (+) or were not (-) preincubated in media containing FGF21 for 2 hours; treatment duration of 30 minutes; PS: Ponceau S.

4. DISCUSSION

This work focused on the characterization of a newly modified murine FGF21 and on how adipose tissue-based organ explants could be used to investigate signaling pathways related to FGF21, insulin and non-selective β-adrenergic receptor agonists. Organ explant culture could be useful to study signal transduction relevant to anabolic pathways such as insulin or to investigate catabolic signal transduction pathways such as lipolysis. Nonetheless, the presented results indicate that it seems to be challenging to induce FGF21 signaling via binding to the FGFR/KLB complexes in adipose organ explants.

Modified murine FGF21 signaling in liver cells

As previously described, the purpose of this thesis was to study a newly developed modFGF21, produced in Pichia pastoris. As a first step, we started to treat HUH7 cells with hFGF19 and in comparison, tested the modFGF21 batches on the cells (Fig. 3). In particular, batch B4 showed the highest increase in phosphorylated ERK1/2 levels.

Yang and coworkers have investigated the role of FGF19 and FGF21 regarding their tissue and receptor specificity. They have demonstrated that FGFR1 and FGFR4 are present in the liver and FGF19 is able to interact with both receptors with high affinity. Further, they have observed that FGF21 can bind with high affinity only to FGFR1 and although binding to the FGFR4/KLB complex was possible, FGF21 could not induce downstream ERK1/2 activation (Yang et al., 2012). Another study contrasts this previous finding. It has shown that FGF21 activates signal transduction by binding to hepatic FGFR4 as well (Adams et al., 2012b). In line with these findings, we saw in our experiment that FGF19 activates phosphorylation of ERK1/2 in HUH7 cells as well. Additionally, we could show that modFGF21 (B4) activates the same signaling cascade as FGF19 and thus, we assume that modFGF21 binds to the complex of KLB and either FGFR1 or FGFR4 in HUH7 cells. However, FGFR1 is predominantly expressed in adipocytes and FGF21 has a stronger binding preference for FGFR1. Therefore, further studies were required to explore effects of modFGF21 in murine adipose tissue.

In this regard, others have already shown that FGF21 induces phosphorylation of MAPK in 3T3-L1 adipocytes using western blot analysis and anti-phospho-ERK1/2 antibodies (Kharitonenkov et al., 2005). Another study from Woolsey and colleagues demonstrated the same effect using human FGF21 on phosphorylated ERK1/2 in HUH7 cells (Woolsey et al., 2016), which is consistent with our data.

The decision to delete the five amino acids of murine modFGF21 was based on the knowledge that human FGF21 is fully biologically active, if the amino acid sequence ΔHPIP is deleted, which was proven in the work of Yie and colleagues from 2009 (Yie et al., 2009). Translated to murine FGF21 (mFGF21), the amino sequence ΔAYPIP has to be deleted and our reported results indicate that the modified version of mFGF21 is able to induce signaling in hepatocytes (Fig. 3). The concept of the drug development was to create an analog with improved half-life in mice compared to the commonly used recombinant versions of human FGF21 in previous trials. Prior research confirmed that mouse plasma contains significantly higher concentration of FAP, the enzyme responsible for FGF21 cleavage (Coppage et al., 2016). Consequently, hFGF21 is degraded significantly faster in mice than in humans and monkeys. Therefore, an improved murine analog could be useful for further investigations of FGF21 effects in mouse models.

Regarding the first attempt to study the effect of modFGF21 on HUH7, we demonstrated that modFGF21 slightly increases *Egr-1* mRNA expression, the downstream target of ERK signaling. This data is in line with the observed increase in protein levels of pERK1/2 after stimulating HUH7cells with modFGF21. These findings indicate that batch B4 activates the FGF21 signaling cascade. Therefore, this batch could be used for further experiments. To this point, it is unclear why the other stocks of modFGF21 (B1, B3 and B6) did not demonstrate similar results in HUH7 liver cells. In particular, B1 impressively decreased *Egr-1* gene expression, indicating antagonistic properties of this batch.

In a previous study, intraperitoneal injection of FGF21 in mice showed increased *Egr-1* expression even after 2 hours (Fisher et al., 2010). Apart from that, *Egr-1* is known as an immediate-early gene and transcription factor with a half-life time of under two hours (Cao et al., 1990, Khachigian, 2023). Although the treatment time

of 30 minutes seems short to show effects on gene expression changes for *Egr-1*, the early growth response gene, published data in other cells suggest that the chosen duration might even be too long (Morawietz et al., 1999). Similarly, the time-points chosen in this study may even missed the peak of phosphorylation of ERK. Taking that into account, it might be possible that a greater *Egr-1* induction might be measured after shorter treatment duration. Thus, further experiments are needed to investigate the effect of different treatment durations on *Egr-1* induction in HUH7 cells.

The use of adipose tissue organ explants to study FGF21 signaling

Previous experiments in our lab were conducted to test recombinant hFGF21 *in vivo* by intraperitoneal injection of C57BL/6 mice with different timepoints and various dosages in fasted and refed animals. hFGF21 increased phosphorylation of ERK1/2 in WAT especially under fasting conditions, compared to vehicle. The effect on phosphorylation of downstream targets in adipose tissue by hFGF21 appears to be dependent on time and the amount of the injected dose, and on whether the animals were fed or fasted (data not shown). In line with this findings, prior research demonstrated that murine 3T3-L1 adipocytes respond to FGF21 within 5 and 60 minutes using low dosage (0,33 nM FGF21) (Ogawa et al., 2007). Another study showed increased ERK activation in 3T3-L1 adipocytes 5 minutes after stimulation with FGF21 (23 nM FGF21) (Minard et al., 2016). ERK activation strongly decreased already 30 minutes after stimulation. In mice intraperitoneal injection with FGF21 resulted in elevated pERK1/2 levels after 5 minutes and interestingly, the protein was almost vanished after 10 minutes (Minard et al., 2016).

To demonstrate the efficacy of hFGF21 in our model, we tested its function in organ explants made of adipose tissue. Furthermore, we tried out treatments with insulin and isoproterenol to investigate if anabolic and catabolic receptor signaling is still inducible in organ explants. For that purpose, we looked at well-known metabolic pathways in adipose tissue. WAT contains triacylglycerol (TAG) as a main energy reserve for humans and animals. When energy deprivation occurs, glycerol and fatty acids are produced by hydrolysis from TAG, which are used as energy substrates

by other organs (Duncan et al., 2007). This process, called lipolysis, was induced by isoproterenol in adipose organ explants and activation of lipolysis was therefore measured by phosphorylation of HSL. Insulin plays an important role in adipose metabolism by stimulating glucose and fatty acid uptake, suppressing lipolysis as an anabolic hormone and inducing *de novo* fatty acid synthesis (Laviola et al., 2006). For that reason, we used insulin in organ explants and measured induced signaling by phosphorylation of Akt.

Regulation of receptor mediated signaling pathways by different hormones

Our previous results indicate that treatment of adipose tissue-based organ explants with isoproterenol increases phosphorylated hormone-sensitive lipase (pHSL) on protein level. Therefore, one can assume that certain extracellular mechanisms of the explants still function *ex vivo*, and treatment induces certain downstream signaling cascades within the cell network. Already decades ago, adipose tissue was treated with isoproterenol to investigate effects on fatty acids synthesis and glucose metabolism (Love et al., 1963). By measuring fatty acid release from adipocytes, an earlier study demonstrated that isoproterenol induces lipolysis in humans and rats (Wenkeova and Wenke, 1970). Hormone-sensitive lipase (HSL) has a crucial enzymatic function in the process of lipolysis, it breaks down diglycerides into fatty acids by hydrolyzation (Schweiger et al., 2014, Holm et al., 2000). Therefore, inducing lipolysis via isoproterenol should lead to PKA-mediated higher phosphorylation levels of HSL, which can be measured using the western blot analysis.

Interestingly, the effect of isoproterenol on phosphorylation of HSL was not affected by the use of different sera, PBS or preincubation with FGF21 in our data. The same applies for the preincubation time, since similar elevation of pHSL was observed after an incubation time of 30 minutes and 8 hours. These findings indicate that b3-adrenergic receptors are still present and able to activate further signal transduction after hours of incubation. Taken together, organ explants from adipose tissue can be used for further research on certain pathways of lipolysis.

Treatment with insulin increases phosphorylation of Akt in organ explants

Similar to FGF21, insulin acts as an endocrine hormone and binds to specific cell-surface receptors with tyrosine kinase activity, that induce intracellular phosphorylation cascades (Laviola et al., 2006). Insulin activates protein kinase B/Akt, which is part of the best-described pathways in insulin signaling and plays a crucial role in insulin-dependent glucose uptake via glucose transporter GLUT4, cell survival and proliferation (Welsh et al., 2005).

In our data, insulin-treatment of adipose organ explants resulted in elevated protein levels of phosphorylated Akt, leading to the assumption that insulin signaling can be activated in the organ explants. Already in 1996, Alessi and colleagues have demonstrated the phosphorylation of Akt by insulin in human embryonic kidney 293 cells on protein level (Alessi et al., 1996). Similar results of phosphorylated Akt have been shown in adipose and liver tissue of rats (Walker et al., 1998), humans and other mammalians (Laviola et al., 2006, Saltiel, 2021). While previous studies have demonstrated similar effects of insulin signaling, up to this point this observation has not yet been described in adipose organ explants.

Similar to the findings from explants treated with isoproterenol, insulin was able to stimulate receptors for the anabolic signaling cascade after 8 hours of incubation. This is supported by the fact that treatment with insulin increased pAKT levels in WAT similarly after an incubation time of 30 minutes and 8 hours. Therefore, we assume that after 8 hours of incubation, receptors for insulin signaling are still present and able to activate further signaling cascades.

FGF21 could not increase pERK1/2 on protein level in organ explants

In previous studies, FGF21 could induce phosphorylation of ERK1/2 in cell culture or *in vivo* in mice (Flippo and Potthoff, 2021). Especially in adipose tissue, the target organ of FGF21, pERK1/2 should be elevated after treatment. However, in our experiments, stimulation with FGF21 did not increase protein levels of pERK1/2 in adipose organ explant culture. The missing induction in this work on adipose organ explant culture could be caused by the following considerations.

Firstly, one important aspect is the experimental set up comprising the time point to treat the explants. The time point in this experiment was chosen inspired by prior studies focusing on FGF21 treatments. Regarding cell experiments *in vitro*, Kharitonenkov and coworkers have proven that FGF21 activates pERK1/2 in 3T3-L1 mouse adipocytes as well as in human adipocytes on protein level. An induction of pERK1/2 could be observed after 2 minutes, while the highest peak was measured between 10 and 30 minutes. Lower pERK1/2 levels were present until 90 minutes after stimulation with FGF21 (Kharitonenkov et al., 2005). In comparison, Ogawa and coworkers induced phosphorylation of ERK1/2 in 3T3-L1 adipocytes between 5 and 60 minutes, with highest increase between 5 and 10 minutes but could not show further induction after 120 minutes (Ogawa et al., 2007). Together, the data indicates that a stimulation with FGF21 has its peak after approximately 10 minutes in mouse adipocytes. For the purpose of studying the induction of pERK1/2, it seems not to be useful to prolong the treatment time because of the already vanished signal of pERK1/2 on immunoblots.

Secondly, we used anti-phospho-ERK antibody covering phosphorylation sites Thr202 and Tyr204 of ERK1/2. It might be possible that another pERK1/2 antibody with phosphorylation site T183/Y185 as used in a study from Minard and coworkers (Minard et al., 2016) is more sensitive for western blot analysis. Future work is required to test the performance of this antibody.

The induction of pERK1/2 through FGF21 is dependent on the presence of KLB and FGFRs (Ogawa et al., 2007). Based on that, an unknown cause of FGF21 resistance, defined as a reduced amount of the receptors FGFR1 and KLB, might have occurred in the set-up. Protein levels of KLB were examined in this work. Unfortunately, some results could not give a clear answer to the question if KLB was still available in a sufficient extent. However, the fact that KLB is still present in various immunoblots of organ explants, is not supporting the idea that missing KLB might be responsible for the missing phosphorylation of EKR1/2. Interestingly, scientists studying effects of KLB downregulation demonstrated that decreased KLB levels did not impair FGF21 signaling in WAT *in vivo* (Markan et al., 2017). Still, protein levels of FGFR1 were not examined in this work and missing FGFR1 might be a possible reason for the missing signal induction.

Because of the previous data generated in our lab, indicating that the nutritional status plays a role in FGF21 signaling, we conducted our experiments with C57BL/6 mice that were either fasted or fasted and refed before organ extraction. The data showed that fasting/refeeding might increase phosphorylation of ERK1/2 over all groups regardless of treatment especially in inguinal but also gonadal WAT. According to the recent findings, we assume that fasting/ refeeding increase the number of available receptors KLB and FGFRs and therefore, improve receptor sensitivity for FGF21 signaling or decrease endogenous mFGF21 that competes for binding with hFGF21 treatment. In northern elephant seals fasting decreased mRNA levels of KLB and FGFR1 in adipose tissue and plasma (Suzuki et al., 2015). Similar to that, KLB expression was downregulated in adipose tissue of fasted mice (Defour et al., 2020), leading to the suggestion that refeeding could induce the opposite effect. However, to test this hypothesis, future research should investigate mRNA expression and protein levels of FGFR1 and KLB in fasting and refeeding models.

An interesting explanation for the improved signal transduction could be that endogenous *mFGF21* gene expression increased in mice after refeeding, and consequently mFGF21 already activated the KLB/FGFR1 complex of WAT in an endocrine manner, which lead to higher induction of pERK1/2 afterwards. This hypothesis is supported by a study, revealing that in mice models fasting and refeeding after 4 hours significantly increased *FGF21* mRNA expression in gonadal WAT (Oishi et al., 2011), in contrast to hepatic FGF21 mRNA levels, which are elevated under fasting conditions (Itoh, 2010).

Nevertheless, at this stage of understanding, fasting/refeeding in the organ explant model could not improve the experimental set-up but demonstrated an important role of the nutritional status in ERK activation.

Since activation of pERK1/2 was seen almost over all groups of the experiments, one can assume that pERK1/2 was induced in all samples before stimulating explants with different treatments. Immediately after the extraction of murine adipose tissue, high levels of pERK1/2 occurred in some samples.

A possible explanation for this observation is provided by the fact, that FGF21 acts as a stress hormone. Thus, *FGF21* gene expression could be induced via endoplasmic reticulum (ER) or mitochondrial stress. In that case, cellular stress could be caused by change in temperature or hypoxia, if organs were not provided with oxygen after euthanizing mice (Oakes and Papa, 2015, Salminen et al., 2017).

Another theory is that the denervation of adipose tissue by surgically removing the fat depots from mice induced phosphorylation of ERK as a possible survival mechanism. This argument is attenuated, however, in that most of the other proteins examined in this work, such as pHSL and pAKT, showed a clear induction after treatment with substances. Further, the protein levels did not change between immediately processed explants and incubated untreated explants.

Charcoal-stripped FBS, dialyzed FBS and PBS did not improve the FGF21 signaling in organ explant culture

Another hypothesis for the missing signal transduction through FGF21 could be that bovine FGF21 from FBS used for incubation did already bind to FGFR1/KLB and receptors were not available on the cell surface during the following treatment with recombinant hFGF21 in our experiments. With the idea of removing components from the media that might saturate the FGFR1/KLB complex, we incubated explants with different sera. Urzì and colleagues have already discussed the negative sides of FBS in cell culture. They have pointed out that FBS is not completely characterized, and it is known to also consist of active hormones such as growth hormone, which might affect FGF21-signaling. Moreover, it can be contaminated by endotoxins, viruses and prions (Urzi et al., 2022). Therefore, the previously described charcoal-stripped FBS or dialyzed FBS were tested in the experimental set-up. Charcoal-stripping of the serum is usually used to remove growth hormones, steroid hormones and cytokines which has been shown to improve different signaling cascades such as MAPK signaling (Dang and Lowik, 2005). Dialyzing of the serum removes substances of low molecular weight such as proteins. Furthermore, organ explants were incubated in PBS, to investigate how the complete loss of proteins affect the organ explants.

The use of csFBS, dFBS or soley PBS for culturing the adipose tissue-based organ explants did not improve the results regarding FGF21 signaling in this work. Therefore, we concluded that the serum is not responsible for the failed increase of pERK1/2. This statement is supported by two facts. Firstly, pAKT and pHSL were induced in explants treated with insulin and isoproterenol, respectively. This fact seems to support the previous hypothesis that sera are not responsible for the ERK induction. However, explants incubated solely in PBS seem to show a slightly improved stimulation by FGF21. Secondly, organ explants directly processed after extraction showed present pERK1/2 levels although they were not incubated in media. Based on that, it might be possible that phosphorylation of ERK1/2 was induced prior to the start of the experiment.

Pretreatment with hFGF21 could not show a clear improvement in FGF21 signaling

As the first experiments using different sera failed to improve our results, we tried to preincubate the organ explants for 2h with FGF21 prior to a second FGF21 incubation step. The idea was to test if the additional preincubation could sensitize the signaling cascades downstream of FG21, assuming that either the receptors are insensitive or the used concentration of FGF21 is not appropriate to induce pERK1/2. Therefore, we hypothesized that preincubation causes a higher binding affinity of FGF21 and thus, stronger induction of pERK1/2, which to this point was never tested before in previous studies.

Surprisingly, in iWAT the additional 2h-incubation seems to increase the amount of pERK1/2. This finding is contradictory to the previously discussed data that shows that pERK1/2 through FGF21 stimulation vanishes after 90 minutes in cell lines. However, the repeated stimulation of the KLB/FGFR1 complex in our experiments seems to improve FGF21 signaling. Further experiments are necessary to examine the role of incubation time and to find answers to why gWAT did not demonstrate equal results (Fig. 21-23).

For a long time, WAT was only seen as an energy storage depot (Steiner and Cahill, 1964). Nevertheless, there are differences between the different fat depots of WAT. Gonadal fat depots belong to the more metabolically active visceral adipose tissue, which is known for its lipolytic potential. Whereas inguinal WAT belongs to the group of subcutaneous WAT that displays less metabolic activity but is known for its function as an energy storage depot (van Beek et al., 2015, Bjorndal et al., 2011). For a better understanding, it would be interesting to conduct experiments comparing the response of iWAT and gWAT to the different treatment stimuli, which could be achieved by bringing the samples together on the same SDS-page gels.

Because this work was defined as a pilot experiment for further studies on the use of modFGF21 and adipose tissue-based organ explants, the findings of this study have to be seen in light of some general limitations. First, certain experiments were performed only once and should be confirmed by repeating the experiments according to the used protocols, to validate our made statements. Secondly, the Ponceau S serving as loading control for our proteins showed uneven protein loading in some of our samples. Since we tried to exclude pipetting mistakes, we assume that lipid contaminants might be responsible for the unequal loadings. The protocol should be adapted to eliminate the lipids. Additional centrifugation steps during the protein isolation could be useful to get pure extraction of the protein section without the disturbing lipids. Furthermore, future research into FGF21 signaling by measuring pERK1/2 should be accompanied by analysis of protein levels of total ERK. The levels of total ERK have to be equal and prove that the total amount of ERK was not changed by different treatments. Finally, the sample size in each group should be increased and statistical analysis should be performed in future studies demonstrating significant results.

Nevertheless, this diploma thesis demonstrates that organ explant culture based on adipose tissue can be utilized to test different signaling cascades in lipid metabolism even though FGF21 could not induce a clear induction of pERK1/2 in adipose explant cultures. Further investigations are needed to develop a system that can be applied to FGF21.

5. REFERENCES

ADAMS, A. C., CHENG, C. C., COSKUN, T. & KHARITONENKOV, A. 2012a. FGF21 requires betaklotho to act in vivo. *PLoS One,* 7**,** e49977.

ADAMS, A. C., COSKUN, T., ROVIRA, A. R., SCHNEIDER, M. A., RACHES, D. W., MICANOVIC, R., BINA, H. A., DUNBAR, J. D. & KHARITONENKOV, A. 2012b. Fundamentals of FGF19 & FGF21 action in vitro and in vivo. *PLoS One,* 7**,** e38438.

ALESSI, D. R., ANDJELKOVIC, M., CAUDWELL, B., CRON, P., MORRICE, N., COHEN, P. & HEMMINGS, B. A. 1996. Mechanism of activation of protein kinase B by insulin and IGF-1. *The EMBO Journal,* 15**,** 6541-6551.

ARNER, P., PETTERSSON, A., MITCHELL, P. J., DUNBAR, J. D., KHARITONENKOV, A. & RYDEN, M. 2008. FGF21 attenuates lipolysis in human adipocytes - a possible link to improved insulin sensitivity. *FEBS Lett,* 582**,** 1725-30.

ASADA, N., TANAKA, Y., HAYASHIDO, Y., TORATANI, S., KAN, M., KITAMOTO, M., NAKANISHI, T., KAJIYAMA, G., CHAYAMA, K. & OKAMOTO, T. 2003. Expression of fibroblast growth factor receptor genes in human hepatoma-derived cell lines. *In Vitro Cell Dev Biol Anim,* 39**,** 321-8.

BADMAN, M. K., PISSIOS, P., KENNEDY, A. R., KOUKOS, G., FLIER, J. S. & MARATOS-FLIER, E. 2007. Hepatic fibroblast growth factor 21 is regulated by PPARalpha and is a key mediator of hepatic lipid metabolism in ketotic states. *Cell Metab,* 5**,** 426-37.

BARUCH, A., WONG, C., CHINN, L. W., VAZE, A., SONODA, J., GELZLEICHTER, T., CHEN, S., LEWIN-KOH, N., MORROW, L., DHEERENDRA, S., BOISMENU, R., GUTIERREZ, J., WAKSHULL, E., WILSON, M. E. & ARORA, P. S. 2020. Antibody-mediated activation of the FGFR1/Klothobeta complex corrects metabolic dysfunction and alters food preference in obese humans. *Proc Natl Acad Sci U S A,* 117**,** 28992-29000.

BEENKEN, A. & MOHAMMADI, M. 2009. The FGF family: biology, pathophysiology and therapy. *Nat Rev Drug Discov,* 8**,** 235-53.

BEENKEN, A. & MOHAMMADI, M. 2012. The structural biology of the FGF19 subfamily. *Adv Exp Med Biol,* 728**,** 1-24.

BERGLUND, E. D., LI, C. Y., BINA, H. A., LYNES, S. E., MICHAEL, M. D., SHANAFELT, A. B., KHARITONENKOV, A. & WASSERMAN, D. H. 2009. Fibroblast growth factor 21 controls glycemia via regulation of hepatic glucose flux and insulin sensitivity. *Endocrinology,* 150**,** 4084-93.

BJORNDAL, B., BURRI, L., STAALESEN, V., SKORVE, J. & BERGE, R. K. 2011. Different adipose depots: their role in the development of metabolic syndrome and mitochondrial response to hypolipidemic agents. *J Obes,* 2011**,** 490650.

BONDURANT, L. D., AMEKA, M., NABER, M. C., MARKAN, K. R., IDIGA, S. O., ACEVEDO, M. R., WALSH, S. A., ORNITZ, D. M. & POTTHOFF, M. J. 2017. FGF21 Regulates Metabolism Through Adipose-Dependent and -Independent Mechanisms. *Cell Metab,* 25**,** 935-944 e4.

BOOKOUT, A. L., DE GROOT, M. H., OWEN, B. M., LEE, S., GAUTRON, L., LAWRENCE, H. L., DING, X., ELMQUIST, J. K., TAKAHASHI, J. S., MANGELSDORF, D. J. & KLIEWER, S. A. 2013. FGF21 regulates metabolism and circadian behavior by acting on the nervous system. *Nat Med,* 19**,** 1147-52.

BYUN, S., SEOK, S., KIM, Y. C., ZHANG, Y., YAU, P., IWAMORI, N., XU, H. E., MA, J., KEMPER, B. & KEMPER, J. K. 2020. Fasting-induced FGF21 signaling activates hepatic autophagy and lipid degradation via JMJD3 histone demethylase. *Nat Commun,* 11**,** 807.

CANTO, C. & AUWERX, J. 2012. Targeting sirtuin 1 to improve metabolism: all you need is NAD(+)? *Pharmacol Rev,* 64**,** 166-87.

CAO, X. M., KOSKI, R. A., GASHLER, A., MCKIERNAN, M., MORRIS, C. F., GAFFNEY, R., HAY, R. V. & SUKHATME, V. P. 1990. Identification and characterization of the Egr-1 gene

product, a DNA-binding zinc finger protein induced by differentiation and growth signals. *Molecular and Cellular Biology,* 10**,** 1931-1939.
CHARTOUMPEKIS, D. V., HABEOS, I. G., ZIROS, P. G., PSYROGIANNIS, A. I., KYRIAZOPOULOU, V. E. & PAPAVASSILIOU, A. G. 2011. Brown adipose tissue responds to cold and adrenergic stimulation by induction of FGF21. *Mol Med,* 17**,** 736-40.
CHAU, M. D., GAO, J., YANG, Q., WU, Z. & GROMADA, J. 2010. Fibroblast growth factor 21 regulates energy metabolism by activating the AMPK-SIRT1-PGC-1alpha pathway. *Proc Natl Acad Sci U S A,* 107**,** 12553-8.
COPPAGE, A. L., HEARD, K. R., DIMARE, M. T., LIU, Y., WU, W., LAI, J. H. & BACHOVCHIN, W. W. 2016. Human FGF-21 Is a Substrate of Fibroblast Activation Protein. *PLoS One,* 11**,** e0151269.
DANG, Z. C. & LOWIK, C. W. 2005. Removal of serum factors by charcoal treatment promotes adipogenesis via a MAPK-dependent pathway. *Mol Cell Biochem,* 268**,** 159-67.
DEFOUR, M., MICHIELSEN, C., O'DONOVAN, S. D., AFMAN, L. A. & KERSTEN, S. 2020. Transcriptomic signature of fasting in human adipose tissue. *Physiol Genomics,* 52**,** 451-467.
DI LISA, F. & ITOH, N. 2015. Cardiac Fgf21 synthesis and release: an autocrine loop for boosting up antioxidant defenses in failing hearts. *Cardiovasc Res,* 106**,** 1-3.
DUNCAN, R. E., AHMADIAN, M., JAWORSKI, K., SARKADI-NAGY, E. & SUL, H. S. 2007. Regulation of lipolysis in adipocytes. *Annu Rev Nutr,* 27**,** 79-101.
DUNSHEE, D. R., BAINBRIDGE, T. W., KLJAVIN, N. M., ZAVALA-SOLORIO, J., SCHROEDER, A. C., CHAN, R., CORPUZ, R., WONG, M., ZHOU, W., DESHMUKH, G., LY, J., SUTHERLIN, D. P., ERNST, J. A. & SONODA, J. 2016. Fibroblast Activation Protein Cleaves and Inactivates Fibroblast Growth Factor 21. *J Biol Chem,* 291**,** 5986-5996.
FALAMARZI, K., MALEKPOUR, M., TAFTI, M. F., AZARPIRA, N., BEHBOODI, M. & ZAREI, M. 2022. The role of FGF21 and its analogs on liver associated diseases. *Front Med (Lausanne),* 9**,** 967375.
FISHER, F. M., CHUI, P. C., ANTONELLIS, P. J., BINA, H. A., KHARITONENKOV, A., FLIER, J. S. & MARATOS-FLIER, E. 2010. Obesity is a fibroblast growth factor 21 (FGF21)-resistant state. *Diabetes,* 59**,** 2781-9.
FISHER, F. M., ESTALL, J. L., ADAMS, A. C., ANTONELLIS, P. J., BINA, H. A., FLIER, J. S., KHARITONENKOV, A., SPIEGELMAN, B. M. & MARATOS-FLIER, E. 2011. Integrated regulation of hepatic metabolism by fibroblast growth factor 21 (FGF21) in vivo. *Endocrinology,* 152**,** 2996-3004.
FLIPPO, K. H. & POTTHOFF, M. J. 2021. Metabolic Messengers: FGF21. *Nat Metab,* 3**,** 309-317.
FON TACER, K., BOOKOUT, A. L., DING, X., KUROSU, H., JOHN, G. B., WANG, L., GOETZ, R., MOHAMMADI, M., KURO-O, M., MANGELSDORF, D. J. & KLIEWER, S. A. 2010. Research resource: Comprehensive expression atlas of the fibroblast growth factor system in adult mouse. *Mol Endocrinol,* 24**,** 2050-64.
GADALETA, R. M. & MOSCHETTA, A. 2019. Metabolic Messengers: fibroblast growth factor 15/19. *Nat Metab,* 1**,** 588-594.
GAICH, G., CHIEN, J. Y., FU, H., GLASS, L. C., DEEG, M. A., HOLLAND, W. L., KHARITONENKOV, A., BUMOL, T., SCHILSKE, H. K. & MOLLER, D. E. 2013. The effects of LY2405319, an FGF21 analog, in obese human subjects with type 2 diabetes. *Cell Metab,* 18**,** 333-40.
GENG, L., LAM, K. S. L. & XU, A. 2020. The therapeutic potential of FGF21 in metabolic diseases: from bench to clinic. *Nat Rev Endocrinol,* 16**,** 654-667.
GENG, L., LIAO, B., JIN, L., HUANG, Z., TRIGGLE, C. R., DING, H., ZHANG, J., HUANG, Y., LIN, Z. & XU, A. 2019. Exercise Alleviates Obesity-Induced Metabolic Dysfunction via Enhancing FGF21 Sensitivity in Adipose Tissues. *Cell Rep,* 26**,** 2738-2752 e4.
GOMEZ-SAMANO, M. A., GRAJALES-GOMEZ, M., ZUARTH-VAZQUEZ, J. M., NAVARRO-FLORES, M. F., MARTINEZ-SAAVEDRA, M., JUAREZ-LEON, O. A., MORALES-GARCIA, M. G., ENRIQUEZ-ESTRADA, V. M., GOMEZ-PEREZ, F. J. & CUEVAS-RAMOS, D. 2017.

Fibroblast growth factor 21 and its novel association with oxidative stress. *Redox Biol,* 11**,** 335-341.
HALUZÍK, M. M. & HALUZÍK, M. 2006. PPAR-alpha and insulin sensitivity. *Physiological Research***,** 115-122.
HARRISON, S. A., RUANE, P. J., FREILICH, B. L., NEFF, G., PATIL, R., BEHLING, C. A., HU, C., FONG, E., DE TEMPLE, B., TILLMAN, E. J., ROLPH, T. P., CHENG, A. & YALE, K. 2021. Efruxifermin in non-alcoholic steatohepatitis: a randomized, double-blind, placebo-controlled, phase 2a trial. *Nat Med,* 27**,** 1262-1271.
HENRIKSSON, E. & ANDERSEN, B. 2020. FGF19 and FGF21 for the Treatment of NASH-Two Sides of the Same Coin? Differential and Overlapping Effects of FGF19 and FGF21 From Mice to Human. *Front Endocrinol (Lausanne),* 11**,** 601349.
HOLM, C., OSTERLUND, T., LAURELL, H. & CONTRERAS, J. A. 2000. Molecular mechanisms regulating hormone-sensitive lipase and lipolysis. *Annu Rev Nutr,* 20**,** 365-93.
HOTTA, Y., NAKAMURA, H., KONISHI, M., MURATA, Y., TAKAGI, H., MATSUMURA, S., INOUE, K., FUSHIKI, T. & ITOH, N. 2009. Fibroblast growth factor 21 regulates lipolysis in white adipose tissue but is not required for ketogenesis and triglyceride clearance in liver. *Endocrinology,* 150**,** 4625-33.
HSUCHOU, H., PAN, W. & KASTIN, A. J. 2007. The fasting polypeptide FGF21 can enter brain from blood. *Peptides,* 28**,** 2382-6.
IIZUKA, K., TAKEDA, J. & HORIKAWA, Y. 2009. Glucose induces FGF21 mRNA expression through ChREBP activation in rat hepatocytes. *FEBS Letters,* 583**,** 2882-2886.
INAGAKI, T., DUTCHAK, P., ZHAO, G., DING, X., GAUTRON, L., PARAMESWARA, V., LI, Y., GOETZ, R., MOHAMMADI, M., ESSER, V., ELMQUIST, J. K., GERARD, R. D., BURGESS, S. C., HAMMER, R. E., MANGELSDORF, D. J. & KLIEWER, S. A. 2007. Endocrine regulation of the fasting response by PPARalpha-mediated induction of fibroblast growth factor 21. *Cell Metab,* 5**,** 415-25.
IROZ, A., MONTAGNER, A., BENHAMED, F., LEVAVASSEUR, F., POLIZZI, A., ANTHONY, E., REGNIER, M., FOUCHE, E., LUKOWICZ, C., CAUZAC, M., TOURNIER, E., DO-CRUZEIRO, M., DAUJAT-CHAVANIEU, M., GERBAL-CHALOUIN, S., FAUVEAU, V., MARMIER, S., BURNOL, A. F., GUILMEAU, S., LIPPI, Y., GIRARD, J., WAHLI, W., DENTIN, R., GUILLOU, H. & POSTIC, C. 2017. A Specific ChREBP and PPARalpha Cross-Talk Is Required for the Glucose-Mediated FGF21 Response. *Cell Rep,* 21**,** 403-416.
ITOH, N. 2010. Hormone-like (endocrine) Fgfs: their evolutionary history and roles in development, metabolism, and disease. *Cell Tissue Res,* 342**,** 1-11.
ITOH, N. & OHTA, H. 2013. Pathophysiological roles of FGF signaling in the heart. *Front Physiol,* 4**,** 247.
KANWAL, F., SHUBROOK, J. H., YOUNOSSI, Z., NATARAJAN, Y., BUGIANESI, E., RINELLA, M. E., HARRISON, S. A., MANTZOROS, C., PFOTENHAUER, K., KLEIN, S., ECKEL, R. H., KRUGER, D., EL-SERAG, H. & CUSI, K. 2021. Preparing for the NASH Epidemic: A Call to Action. *Gastroenterology,* 161**,** 1030-1042 e8.
KAUR, N., GARE, S. R., SHEN, J., RAJA, R., FONSEKA, O. & LIU, W. 2022. Multi-organ FGF21-FGFR1 signaling in metabolic health and disease. *Front Cardiovasc Med,* 9**,** 962561.
KE, Y., XU, C., LIN, J. & LI, Y. 2019. Role of Hepatokines in Non-alcoholic Fatty Liver Disease. *J Transl Int Med,* 7**,** 143-148.
KEINICKE, H., SUN, G., MENTZEL, C. M. J., FREDHOLM, M., JOHN, L. M., ANDERSEN, B., RAUN, K. & KJAERGAARD, M. 2020. FGF21 regulates hepatic metabolic pathways to improve steatosis and inflammation. *Endocr Connect,* 9**,** 755-768.
KHACHIGIAN, L. M. 2023. The MEK-ERK-Egr-1 axis and its regulation in cardiovascular disease. *Vascul Pharmacol,* 153**,** 107232.
KHARITONENKOV, A., SHIYANOVA, T. L., KOESTER, A., FORD, A. M., MICANOVIC, R., GALBREATH, E. J., SANDUSKY, G. E., HAMMOND, L. J., MOYERS, J. S., OWENS, R. A., GROMADA, J., BROZINICK, J. T., HAWKINS, E. D., WROBLEWSKI, V. J., LI, D. S.,

MEHRBOD, F., JASKUNAS, S. R. & SHANAFELT, A. B. 2005. FGF-21 as a novel metabolic regulator. *J Clin Invest,* 115**,** 1627-35.
KIM, K. H. & LEE, M. S. 2015. FGF21 as a mediator of adaptive responses to stress and metabolic benefits of anti-diabetic drugs. *J Endocrinol,* 226**,** R1-16.
KUROSU, H., CHOI, M., OGAWA, Y., DICKSON, A. S., GOETZ, R., ELISEENKOVA, A. V., MOHAMMADI, M., ROSENBLATT, K. P., KLIEWER, S. A. & KURO, O. M. 2007. Tissue-specific expression of betaKlotho and fibroblast growth factor (FGF) receptor isoforms determines metabolic activity of FGF19 and FGF21. *J Biol Chem,* 282**,** 26687-26695.
LAEGER, T., HENAGAN, T. M., ALBARADO, D. C., REDMAN, L. M., BRAY, G. A., NOLAND, R. C., MUNZBERG, H., HUTSON, S. M., GETTYS, T. W., SCHWARTZ, M. W. & MORRISON, C. D. 2014. FGF21 is an endocrine signal of protein restriction. *J Clin Invest,* 124**,** 3913-22.
LAN, T., MORGAN, D. A., RAHMOUNI, K., SONODA, J., FU, X., BURGESS, S. C., HOLLAND, W. L., KLIEWER, S. A. & MANGELSDORF, D. J. 2017. FGF19, FGF21, and an FGFR1/beta-Klotho-Activating Antibody Act on the Nervous System to Regulate Body Weight and Glycemia. *Cell Metab,* 26**,** 709-718 e3.
LAVIOLA, L., PERRINI, S., CIGNARELLI, A. & GIORGINO, F. 2006. Insulin signalling in human adipose tissue. *Arch Physiol Biochem,* 112**,** 82-8.
LEE, S., CHOI, J., MOHANTY, J., SOUSA, L. P., TOME, F., PARDON, E., STEYAERT, J., LEMMON, M. A., LAX, I. & SCHLESSINGER, J. 2018. Structures of beta-klotho reveal a 'zip code'-like mechanism for endocrine FGF signalling. *Nature,* 553**,** 501-505.
LIANG, Q., ZHONG, L., ZHANG, J., WANG, Y., BORNSTEIN, S. R., TRIGGLE, C. R., DING, H., LAM, K. S. & XU, A. 2014. FGF21 maintains glucose homeostasis by mediating the cross talk between liver and brain during prolonged fasting. *Diabetes,* 63**,** 4064-75.
LIU, S. Q., ROBERTS, D., KHARITONENKOV, A., ZHANG, B., HANSON, S. M., LI, Y. C., ZHANG, L. Q. & WU, Y. H. 2013. Endocrine protection of ischemic myocardium by FGF21 from the liver and adipose tissue. *Sci Rep,* 3**,** 2767.
LOVE, W. C., CARR, L. & ASHMORE, J. 1963. Influence of Isoproterenol and 1-(2'-4'-Dichlorophenyl)-2-t-Butylaminoethanol (DCB) on Free Fatty Acid Release and Glucose Metabolism in Adipose Tissue. *Pharmacol Exp Ther,* 142**,** 137-140.
LUO, Y., YE, S., LI, X. & LU, W. 2019. Emerging Structure-Function Paradigm of Endocrine FGFs in Metabolic Diseases. *Trends Pharmacol Sci,* 40**,** 142-153.
MARKAN, K. R., NABER, M. C., AMEKA, M. K., ANDEREGG, M. D., MANGELSDORF, D. J., KLIEWER, S. A., MOHAMMADI, M. & POTTHOFF, M. J. 2014. Circulating FGF21 is liver derived and enhances glucose uptake during refeeding and overfeeding. *Diabetes,* 63**,** 4057-63.
MARKAN, K. R., NABER, M. C., SMALL, S. M., PELTEKIAN, L., KESSLER, R. L. & POTTHOFF, M. J. 2017. FGF21 resistance is not mediated by downregulation of beta-klotho expression in white adipose tissue. *Mol Metab,* 6**,** 602-610.
MATSUI, S., SASAKI, T., KOHNO, D., YAKU, K., INUTSUKA, A., YOKOTA-HASHIMOTO, H., KIKUCHI, O., SUGA, T., KOBAYASHI, M., YAMANAKA, A., HARADA, A., NAKAGAWA, T., ONAKA, T. & KITAMURA, T. 2018. Neuronal SIRT1 regulates macronutrient-based diet selection through FGF21 and oxytocin signalling in mice. *Nat Commun,* 9**,** 4604.
MINARD, A. Y., TAN, S. X., YANG, P., FAZAKERLEY, D. J., DOMANOVA, W., PARKER, B. L., HUMPHREY, S. J., JOTHI, R., STOCKLI, J. & JAMES, D. E. 2016. mTORC1 Is a Major Regulatory Node in the FGF21 Signaling Network in Adipocytes. *Cell Rep,* 17**,** 29-36.
MOHAMMADI, M., DIKIC, I., SOROKIN, A., BURGESS, W. H., JAYE, M. & SCHLESSINGER, J. 1996. Identification of six novel autophosphorylation sites on fibroblast growth factor receptor 1 and elucidation of their importance in receptor activation and signal transduction. *Mol Cell Biol,* 16**,** 977-89.
MORAWIETZ, H., MA, Y. H., VIVES, F., WILSON, E., SUKHATME, V. P., HOLTZ, J. & IVES, H. E. 1999. Rapid induction and translocation of Egr-1 in response to mechanical strain in vascular smooth muscle cells. *Circ Res,* 84**,** 678-87.

NISHIMURA, T., NAKATAKE, Y., KONISHI, M. & ITOH, N. 2000. Identification of a novel FGF, FGF-21, preferentially expressed in the liver. *Biochim Biophys Acta,* 1492**,** 203-6.
OAKES, S. A. & PAPA, F. R. 2015. The role of endoplasmic reticulum stress in human pathology. *Annu Rev Pathol,* 10**,** 173-94.
OGAWA, Y., KUROSU, H., YAMAMOTO, M., NANDI, A., ROSENBLATT, K. P., GOETZ, R., ELISEENKOVA, A. V., MOHAMMADI, M. & KURO-O, M. 2007. BetaKlotho is required for metabolic activity of fibroblast growth factor 21. *Proc Natl Acad Sci U S A,* 104**,** 7432-7.
OISHI, K., KONISHI, M., MURATA, Y. & ITOH, N. 2011. Time-imposed daily restricted feeding induces rhythmic expression of Fgf21 in white adipose tissue of mice. *Biochem Biophys Res Commun,* 412**,** 396-400.
ORNITZ, D. M. & ITOH, N. 2001. Fibroblast growth factors. *Genome Biol,* 2**,** REVIEWS3005.
OWEN, B. M., DING, X., MORGAN, D. A., COATE, K. C., BOOKOUT, A. L., RAHMOUNI, K., KLIEWER, S. A. & MANGELSDORF, D. J. 2014. FGF21 acts centrally to induce sympathetic nerve activity, energy expenditure, and weight loss. *Cell Metab,* 20**,** 670-7.
PATEL, V., ADYA, R., CHEN, J., RAMANJANEYA, M., BARI, M. F., BHUDIA, S. K., HILLHOUSE, E. W., TAN, B. K. & RANDEVA, H. S. 2014. Novel insights into the cardio-protective effects of FGF21 in lean and obese rat hearts. *PLoS One,* 9**,** e87102.
PLANAVILA, A., REDONDO, I., HONDARES, E., VINCIGUERRA, M., MUNTS, C., IGLESIAS, R., GABRIELLI, L. A., SITGES, M., GIRALT, M., VAN BILSEN, M. & VILLARROYA, F. 2013. Fibroblast growth factor 21 protects against cardiac hypertrophy in mice. *Nat Commun,* 4**,** 2019.
POTTHOFF, M. J., INAGAKI, T., SATAPATI, S., DING, X., HE, T., GOETZ, R., MOHAMMADI, M., FINCK, B. N., MANGELSDORF, D. J., KLIEWER, S. A. & BURGESS, S. C. 2009. FGF21 induces PGC-1alpha and regulates carbohydrate and fatty acid metabolism during the adaptive starvation response. *Proc Natl Acad Sci U S A,* 106**,** 10853-8.
RADER, D. J., MARATOS-FLIER, E., NGUYEN, A., HOM, D., FERRIERE, M., LI, Y., KOMPA, J., MARTIC, M., HINDER, M., BASSON, C. T., YOWE, D., DIENER, J., GOLDFINE, A. B. & TEAM, C. X. S. 2022. LLF580, an FGF21 Analog, Reduces Triglycerides and Hepatic Fat in Obese Adults With Modest Hypertriglyceridemia. *J Clin Endocrinol Metab,* 107**,** e57-e70.
RESAU, J. H., SAKAMOTO, K., COTTRELL, J. R., HUDSON, E. A. & MELTZER, S. J. 1991. Explant organ culture: a review. *Cytotechnology,* 7**,** 137-49.
RUSLI, F., DEELEN, J., ANDRIYANI, E., BOEKSCHOTEN, M. V., LUTE, C., VAN DEN AKKER, E. B., MULLER, M., BEEKMAN, M. & STEEGENGA, W. T. 2016. Fibroblast growth factor 21 reflects liver fat accumulation and dysregulation of signalling pathways in the liver of C57BL/6J mice. *Sci Rep,* 6**,** 30484.
SAELY, C. H., GEIGER, K. & DREXEL, H. 2012. Brown versus white adipose tissue: a mini-review. *Gerontology,* 58**,** 15-23.
SALMINEN, A., KAARNIRANTA, K. & KAUPPINEN, A. 2017. Regulation of longevity by FGF21: Interaction between energy metabolism and stress responses. *Ageing Res Rev,* 37**,** 79-93.
SALTIEL, A. R. 2021. Insulin signaling in health and disease. *J Clin Invest,* 131.
SANYAL, A., CHARLES, E. D., NEUSCHWANDER-TETRI, B. A., LOOMBA, R., HARRISON, S. A., ABDELMALEK, M. F., LAWITZ, E. J., HALEGOUA-DEMARZIO, D., KUNDU, S., NOVIELLO, S., LUO, Y. & CHRISTIAN, R. 2019. Pegbelfermin (BMS-986036), a PEGylated fibroblast growth factor 21 analogue, in patients with non-alcoholic steatohepatitis: a randomised, double-blind, placebo-controlled, phase 2a trial. *Lancet,* 392**,** 2705-2717.
SCHEELE, C. & WOLFRUM, C. 2020. Brown Adipose Crosstalk in Tissue Plasticity and Human Metabolism. *Endocr Rev,* 41**,** 53-65.
SCHWEIGER, M., EICHMANN, T. O., TASCHLER, U., ZIMMERMANN, R., ZECHNER, R. & LASS, A. 2014. Measurement of lipolysis. *Methods Enzymol,* 538**,** 171-93.
SHE, Q. Y., BAO, J. F., WANG, H. Z., LIANG, H., HUANG, W., WU, J., ZHONG, Y., LING, H., LI, A. & QIN, S. L. 2022. Fibroblast growth factor 21: A "rheostat" for metabolic regulation? *Metabolism,* 130**,** 155166.

STEINER, G. & CAHILL, G. F., JR. 1964. Brown and White Adipose Tissue Metabolism in Cold-Exposed Rats. *Am J Physiol,* 207**,** 840-4.
SUZUKI, M., LEE, A. Y., VAZQUEZ-MEDINA, J. P., VISCARRA, J. A., CROCKER, D. E. & ORTIZ, R. M. 2015. Plasma FGF21 concentrations, adipose fibroblast growth factor receptor-1 and beta-klotho expression decrease with fasting in northern elephant seals. *Gen Comp Endocrinol,* 216**,** 86-9.
SUZUKI, M., UEHARA, Y., MOTOMURA-MATSUZAKA, K., OKI, J., KOYAMA, Y., KIMURA, M., ASADA, M., KOMI-KURAMOCHI, A., OKA, S. & IMAMURA, T. 2008. betaKlotho is required for fibroblast growth factor (FGF) 21 signaling through FGF receptor (FGFR) 1c and FGFR3c. *Mol Endocrinol,* 22**,** 1006-14.
SZCZEPANSKA, E. & GIETKA-CZERNEL, M. 2022. FGF21: A Novel Regulator of Glucose and Lipid Metabolism and Whole-Body Energy Balance. *Horm Metab Res,* 54**,** 203-211.
TALUKDAR, S. & KHARITONENKOV, A. 2021. FGF19 and FGF21: In NASH we trust. *Mol Metab,* 46**,** 101152.
TALUKDAR, S., ZHOU, Y., LI, D., ROSSULEK, M., DONG, J., SOMAYAJI, V., WENG, Y., CLARK, R., LANBA, A., OWEN, B. M., BRENNER, M. B., TRIMMER, J. K., GROPP, K. E., CHABOT, J. R., ERION, D. M., ROLPH, T. P., GOODWIN, B. & CALLE, R. A. 2016. A Long-Acting FGF21 Molecule, PF-05231023, Decreases Body Weight and Improves Lipid Profile in Non-human Primates and Type 2 Diabetic Subjects. *Cell Metab,* 23**,** 427-40.
TREFTS, E., GANNON, M. & WASSERMAN, D. H. 2017. The liver. *Curr Biol,* 27**,** R1147-R1151.
URZI, O., BAGGE, R. O. & CRESCITELLI, R. 2022. The dark side of foetal bovine serum in extracellular vesicle studies. *J Extracell Vesicles,* 11**,** e12271.
VAN BEEK, L., VAN KLINKEN, J. B., PRONK, A. C., VAN DAM, A. D., DIRVEN, E., RENSEN, P. C., KONING, F., WILLEMS VAN DIJK, K. & VAN HARMELEN, V. 2015. The limited storage capacity of gonadal adipose tissue directs the development of metabolic disorders in male C57Bl/6J mice. *Diabetologia,* 58**,** 1601-9.
VON HOLSTEIN-RATHLOU, S., BONDURANT, L. D., PELTEKIAN, L., NABER, M. C., YIN, T. C., CLAFLIN, K. E., URIZAR, A. I., MADSEN, A. N., RATNER, C., HOLST, B., KARSTOFT, K., VANDENBEUCH, A., ANDERSON, C. B., CASSELL, M. D., THOMPSON, A. P., SOLOMON, T. P., RAHMOUNI, K., KINNAMON, S. C., PIEPER, A. A., GILLUM, M. P. & POTTHOFF, M. J. 2016. FGF21 Mediates Endocrine Control of Simple Sugar Intake and Sweet Taste Preference by the Liver. *Cell Metab,* 23**,** 335-43.
WALKER, K. S., DEAK, M., PATERSON, A., HUDSON, K., COHEN, P. & ALESSI, D. R. 1998. Activation of protein kinase B beta and gamma isoforms by insulin in vivo and by 3-phosphoinositide-dependent protein kinase-1 in vitro: comparison with protein kinase B alpha. *Biochem J,* 331 (Pt 1)**,** 299-308.
WELSH, G. I., HERS, I., BERWICK, D. C., DELL, G., WHERLOCK, M., BIRKIN, R., LENEY, S. & TAVARE, J. M. 2005. Role of protein kinase B in insulin-regulated glucose uptake. *Biochem Soc Trans,* 33**,** 346-9.
WENKEOVA, J. & WENKE, M. 1970. In vitro effects of isoproterenol and propranolol on human adipose tissue. *Life Sci,* 9**,** 233-9.
WOOLSEY, S. J., BEATON, M. D., MANSELL, S. E., LEON-PONTE, M., YU, J., PIN, C. L., ADAMS, P. C., KIM, R. B. & TIRONA, R. G. 2016. A Fibroblast Growth Factor 21-Pregnane X Receptor Pathway Downregulates Hepatic CYP3A4 in Nonalcoholic Fatty Liver Disease. *Mol Pharmacol,* 90**,** 437-46.
XU, J., LLOYD, D. J., HALE, C., STANISLAUS, S., CHEN, M., SIVITS, G., VONDERFECHT, S., HECHT, R., LI, Y. S., LINDBERG, R. A., CHEN, J. L., JUNG, D. Y., ZHANG, Z., KO, H. J., KIM, J. K. & VENIANT, M. M. 2009a. Fibroblast growth factor 21 reverses hepatic steatosis, increases energy expenditure, and improves insulin sensitivity in diet-induced obese mice. *Diabetes,* 58**,** 250-9.
XU, J., STANISLAUS, S., CHINOOKOSWONG, N., LAU, Y. Y., HAGER, T., PATEL, J., GE, H., WEISZMANN, J., LU, S. C., GRAHAM, M., BUSBY, J., HECHT, R., LI, Y. S., LI, Y., LINDBERG, R. & VENIANT, M. M. 2009b. Acute glucose-lowering and insulin-sensitizing

action of FGF21 in insulin-resistant mouse models--association with liver and adipose tissue effects. *Am J Physiol Endocrinol Metab,* 297**,** E1105-14.

YANG, C., JIN, C., LI, X., WANG, F., MCKEEHAN, W. L. & LUO, Y. 2012. Differential specificity of endocrine FGF19 and FGF21 to FGFR1 and FGFR4 in complex with KLB. *PLoS One,* 7**,** e33870.

YAQOOB, U., JAGAVELU, K., SHERGILL, U., DE ASSUNCAO, T., CAO, S. & SHAH, V. H. 2014. FGF21 promotes endothelial cell angiogenesis through a dynamin-2 and Rab5 dependent pathway. *PLoS One,* 9**,** e98130.

YIE, J., HECHT, R., PATEL, J., STEVENS, J., WANG, W., HAWKINS, N., STEAVENSON, S., SMITH, S., WINTERS, D., FISHER, S., CAI, L., BELOUSKI, E., CHEN, C., MICHAELS, M. L., LI, Y. S., LINDBERG, R., WANG, M., VENIANT, M. & XU, J. 2009. FGF21 N- and C-termini play different roles in receptor interaction and activation. *FEBS Lett,* 583**,** 19-24.

ZAREI, M., PIZARRO-DELGADO, J., BARROSO, E., PALOMER, X. & VAZQUEZ-CARRERA, M. 2020. Targeting FGF21 for the Treatment of Nonalcoholic Steatohepatitis. *Trends Pharmacol Sci,* 41**,** 199-208.

ZHU, S., WU, Y., YE, X., MA, L., QI, J., YU, D., WEI, Y., LIN, G., REN, G. & LI, D. 2016. FGF21 ameliorates nonalcoholic fatty liver disease by inducing autophagy. *Mol Cell Biochem,* 420**,** 107-19.